Université de Montréal

Hydrophobically - Modified Hydroxypropyl Celluloses: Synthesis and Self - Assembly in Water

Par

Mariella Piredda

Sciences Pharmaceutiques

Faculté de Pharmacie

Mémoire présenté à la Faculté des études supérieures

En vue de l'obtention du grade de

Maître ès Sciences (M. Sc.)

En sciences pharmaceutiques

Option Chimie médicinale

Avril, 2004

Université de Montréal
Faculté des études supérieures

Ce mémoire intitulé :

Hydrophobically - Modified Hydroxypropyl Cellulose: Synthesis and Self - Assembly in Aqueous Media

Présenté par :
Mariella Piredda

A été évalué par un jury composé des personnes suivantes:

Suzanne Giasson
Président-rapporteur

Géraldine Bazuin
Membre du Jury

Françoise M. Winnik
Directeur de recherche

Mémoire accepté le : 8 avril 2004

RÉSUMÉ

Une série de polymères semi flexibles greffés dans lesquels la partie hydrophobe est distribuée d'une façon statistique le long de l'unité de l'anhydroglucose- a été synthétisée à partir de l'hydroxypropyl cellulose (HPC), du polyoxyéthylène (10) cétyl éther (POE_{10}-C_{16}; Brij-56®), du polyoxyéthylène (20) cétyl éther (POE_{20}-C_{16}; Brij-58®) et du polyoxyéthylène (20) stéaryle éther (POE_{20}-C_{18}; Brij-78®). Les caractérisations physiques et chimiques des polymères modifiés hydrophobiquement sont décrites. La spectroscopie RMN du proton a été utilisée pour déterminer la quantité de Brij conjugué avec les polymères hydrophiles.

Ce type de polymères comportant une partie hydrophile et une partie hydrophobe peut former des micelles, ceci étant dû à leur caractère amphiphile. Ainsi la partie hydrophobe forme le cœur de la micelle et la partie hydrophile entourant ce cœur lui permet de s'hydrater en milieu hydrophile. Ce système permet à la micelle de transporter et de délivrer des médicaments pauvrement solubles dans l'eau. Tant que le cœur hydrophobe peut servir comme micro réservoir pour le médicament, ce dernier sera séparé du milieu par les parties hydrophiles de la micelle. La spectroscopie par fluorescence et la technique de la diffusion de la lumière ont permis la détermination de la dimension des agrégats des micelles polymériques en milieu aqueux. Le fait que les micelles polymériques soient solubles dans l'eau nous a permis d'étudier, avec succès, par DSC (microcalorimétrie thermique différentielle) les propriétés en solution de ces polymères hydrophobiquement modifiés, ainsi que de déterminer leur point de turbidité en fonction du taux de Brij. Du fait que l'HPC porte des groupements fonctionnels, elle pourrait avoir différentes applications dans les domaines biomédicaux comme la libération des médicaments, les diagnostics et la modification des surfaces à travers le couplage des substances bioactives.

Mots clés: HPC, Polysaccharides, micelles polymériques, polymères-HM, libération des médicaments, spectroscopie, diffusion de la lumière, calorimétrie.

ABSTRACT

A series of grafted semiflexible polymers, in which the hydrophobic side chains were located randomly along the anhydroglucose unit, were synthesized by reacting Hydroxypropyl cellulose (HPC) with polyoxyethylene (10) cetyl ether (POE_{10}-C_{16}; Brij-56®), polyoxyethylene (20) cetyl ether (POE_{20}-C_{16}; Brij-58®) and polyoxyethylene (20) stearyl ether (POE_{20}-C_{18}; Brij-78®). The physical and chemical characterization of Hydrophobically Modified (HM) - Polymers is described. 1H-NMR spectroscopy was used for a quantitative determination of the level of Brij® conjugation onto water-soluble polymers. Such systems composed of hydrophilic and hydrophobic segments can form a micellar structure as a result of their amphiphilic character. The hydrophobic segment forms the hydrophobic core of the micelle, and the hydrophilic segment surrounds this core as a hydrated outer shell. This core-shell structure provides polymeric micelles with the potential for use as vehicles for drug delivery, since the hydrophobic core may serve as a microreservoir for drugs, which are segregated from the outer environment by hydrophilic segments. Considerable discussions are made on the physicochemical characteristic of polymeric micelles and dimension of the aggregates in aqueous milieu by Fluorescence spectroscopy and Dynamic Light Scattering techniques. One of the favourable characteristics of polymeric micelles is the water-solubility: Differential Scanning Calorimetry (DSC) was successfully employed to study the solution properties of the HM-polymers to determine their cloud points and elucidate the effects of Brij® content. Functionalized HPC is expected to have a wide utility in biomedical applications such as drug delivery, diagnosis, and surface modification through the coupling of bioactive substances

Keywords: HPC, Polysaccharides, Polymeric micelles, HM-polymers, Drug delivery, Spectroscopy, Dynamic light scattering, Calorimetry.

TABLE OF CONTENTS

LIST OF TABLES

LIST OF FIGURES

LIST OF ^{1}H-NMR SPECTRA

LIST OF FLUORESCENCE PLOTS

LIST OF DSC THERMOGRAMS

ABBREVIATIONS

^{1}H-NMR	Proton Nuclear Magnetic Resonance
ΔH	Enthalpy of transition
CAC	Critical Aggregation Concentration
CH_2Cl_2	Methylene chloride
$CDCl_3$	Chloroform deuterated
CMC	Critical Micellar Concentration
C_p	Molar Heat Capacity
CsA	Cyclosporin A
DLS	Dynamic Light Scattering
DMF	Dimethylformamide
DMSO	Dimethylsulfoxide
DS	Degree of Substitution
DSC	Differential Scanning Calorimetry
GPC	Gel Permeation Chromatography
HCl	Chloridric acid
HM-HPC	Hydrophobically Modified HPC
HPC	Hydroxypropyl cellulose
HPLC	High Performance Liquid Chromatography
LCST	Lower Critical Solution Temperature
MS	Molar Substitution
N_{agg}	Aggregation Number
NaH	Sodium hydroxyde
PAHs	Polycyclic Aromatic Hydrocarbons
Py	Pyrene
POE	Polyoxyethylene
RES	Reticuloendothelial System
SD	Standard Deviation
TEA	Triethylamine
THP	Tetrahydrofuran

TsCl	Tosyl chloride
Tos	Tosylate
UV	Ultraviolet

CHAPTER 1

Introduction

With the rapid progress of biotechnology, peptide drugs have become important therapeutic agents. A wide variety of peptides have been used as drugs, including hormones, synthetic peptides, enzymes substrates, and inhibitors[1]. Although they are highly potent and specific in their physiological functions, most peptides are difficult to administer orally because of their unique physicochemical properties. These include large molecular weight, poor solubility in aqueous media, short plasma half-life, requirement for unique mechanisms for membrane transport, and susceptibility to enzymatic breakdown[2]. Many different approaches have been used to improve the oral absorption and enhance the bioavailability of peptide drugs. In recent years, enhanced bioavailability after oral administration has been observed upon entrapping the drug in a wide variety of polymer particulate carriers which protect the active molecules against inactivation by the host and control drug release in body fluids, *e.g.*, blood, lymph and digestive juice[3].

Microspheres[4,5] and liposomes[6,7] have been devised as delivery systems for the controlled release of vaccines, cytostatics and insulin with special attention to achieving long circulation in the blood stream, and avoiding the RES (reticuloendothelial system) scavenging mechanism. However, the reticuloendothelial system (mainly liver and spleen) actively removes a great majority of these spheres when they are injected. Due to this scavenging, effective delivery of microspheres to organs other than those of the RES is often difficult to achieve.

Thus, several problems, such as biodistribution of drugs, drug solubility, undesirable side effects, rapid clearance by the RES, thermal instability, structurally fragile and low-loading efficiency still exist[8]. New technologies for the preparation of nanosized biodegradable polymeric particles are still required for providing more effective and selective drug delivery systems[9-14].

1.1 Polymeric Micelles

Graft and block copolymers under selective solvent conditions (good solvent for one block and non-solvent for the other block) adopt various organized structures known as "polymeric micelles"[15-21]. Micelles formed by block or graft copolymers belong to the family of colloidal systems.

Polymer micelles have been the subject of growing scientific and industrial interest for their potential biomedical and pharmaceutical applications, such as drug delivery[18,22-31], diagnostics[32], separation technology[33], as well as electronics and optical technologies[34,35]. In particular, in the field of drug delivery, extensive studies have been carried out by many research groups, proposing to use polymer micelles as a novel carrier system for hydrophobic drugs. Many kinds of polymers that form various aggregates in water have been used for this purpose[36-40].

Polymeric micelles result from the association of amphiphilic polymers in water. They are in a mesoscopic size range (several tens of nanometers to 100 nanometers) having a characteristic core-shell architecture, in which the solvophilic segments of the copolymer form an outer shell surrounding the inner core composed of solvophobic segments[41-44]. The core may be utilized as a reservoir of solvophobic compounds which are segregated from the outer environment. This hydrophobic environment possesses potential uses, for example it suppresses the inactivation of drugs molecules by decreasing contact with inactivating species in the aqueous phase (*e.g.* water, specific enzymes), and it controls the drug release by micelle stability and micelle-core hydrophobicity[45]. The outer shell is responsible for the interaction with biocomponents such as proteins and cells, which may determine the pharmacokinetic behaviour and the biodistribution of drugs. Thus, *in vivo* delivery of drugs may be controlled by the outer-shell segment independently of the inner core of the micelle, which expresses pharmacological activities.

By utilizing polymeric micelles, a unique delivery system may be constructed. Independently of drugs bound to the inner core, factors determining the

pharmacokinetic behaviour and biodistribution of polymeric micelles are the chemical characteristics of the outer shell, the water solubility and stability of the micelles.

Because a large number of drugs have a hydrophobic character, a concept very simple and fascinating was to coupling the drug with the carrier in order to deliver the drug by a carrier that had a specific affinity to the organs, tissues, and cells. But conjugation of the drug with a polymer easily leads to precipitation because of the high and localized concentration of the hydrophobic drug molecules bound along the polymer chains. Thus, polymeric micelles were developed with a core-shell structure, which may maintain their water solubility by inhibiting intermicellar aggregation of the hydrophobic cores, irrespective of high hydrophobicity of the inner cores. Furthermore, since interactions among the hydrophobic segments are the driving force in the formation of micelles, the strength of that interaction determines their stability. Compared to low-molecular weight surfactant micelles, polymeric micelles are generally more stable because they self-assembly at much lower concentration, and show slower dissociation which allows longer retention of loaded drugs and higher drug accumulation at the target site[22,46].

The use of polymeric micelles as oral delivery carriers systems has two specific advantages: the first is their size, with diameters in the range of approximately 10-100 nm, which is considered appropriate for evading renal excretion and non-specific capture by the RES. The second advantage includes the protection of the incorporated drug from the aggressive conditions present in the gastrointestinal tract.

In summary, drugs with a hydrophobic character can be easily incorporated into the inner core by physical entrapment[47-51] using experimental methods such as dialysis, salting out process, or solvent evaporation method[3]. Physical entrapment utilizing hydrophobic interaction can be applied to many kinds of drugs, since most drugs possess hydrophobic moiety(ies) in their chemical structure[52]. Some reported advantages of these systems include reduced toxic side effects, solubilization of

hydrophobic drugs, stable storage, bio-distribution, and lower interactions with RES[53-56].

Based on these considerations, our hypothesis was to create an array of materials with controllable, predictable characteristics such as water solubility and ability to encapsulate or solubilize hydrophobic drugs. We expected that water solubility and encapsulation ability would be determined by the ratio of hydrophobic, alkyl chains located in the polymer core relative to the hydrophilic segments at the polymer shell. Since the structural design of the amphiphilic graft copolymer is key in determining the stability of the micelles and their drug-releasing properties, modifying the hydrophobic characteristics of the copolymer may provide micelles with high stability and the most desirable drug-releasing profile[57];

1.2 Hydrophobically Modified (HM)-Cellulose Ethers

Cellulose is a natural polymer and the chief component of wood and plant fibres. Cotton, for example, is almost pure cellulose. Cellulose is a polysaccharide composed of individual anhydroglucose (AHG) units which are held together by ß-1,4 glycoside linkages which make cellulose a long rigid molecule.

Pure cellulose has large crystalline regions due to hydrogen bonds between the -OH groups on different chains (Figure 1.1).

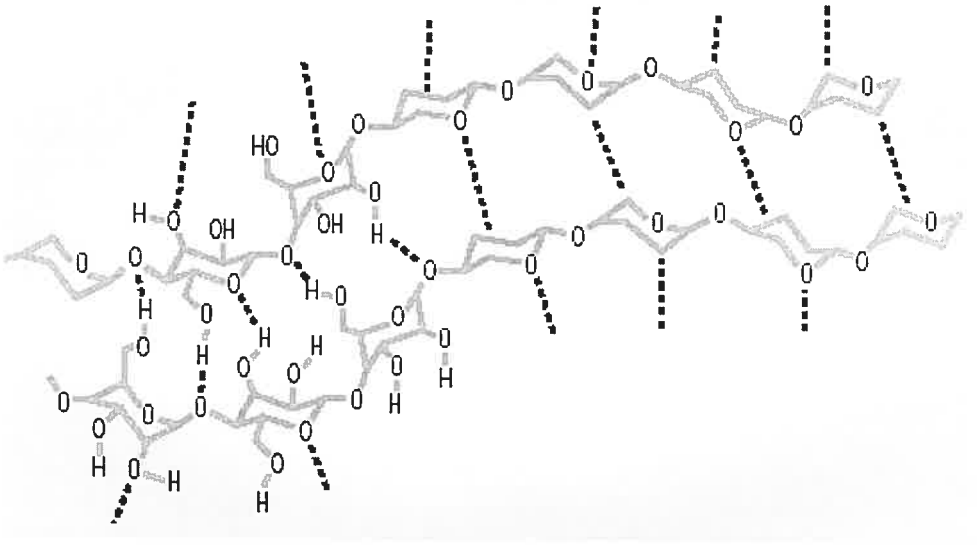

Figure 1.1. Cellulose hydrogen bonds keep adjacent chains together

In the manufacturing of cellulose ethers, purified cellulose is activated in a first step with sodium hydroxide solution. In this alkalisation reaction, the structures of the crystalline areas are expanded allowing the hydroxyl groups to be transformed into alcoholate (this cellulose alcoholate is termed alkali cellulose). The strong attractive forces between cellulose chains due to interchain hydrogen bonds will be greatly reduced by alkylating the greater portion of the -OH groups, thereby preventing hydrogen bonding. Such chemical modification results in significantly changed characteristics with regard to solubility, surface activity, chemical resistance and enzyme resistance. In this way it is possible to produce sets of cellulose ethers with carefully calculated performance characteristics. The properties of the cellulose ether are determined by the type of substituents, and also by their number and distribution along the molecule chain.

Cellulose ethers have a broad range of industrial applications. They are used as additives in materials such as paints, inks, papers, cosmetics, pharmaceuticals, foods and ceramics. Their solution properties are dictated mostly by the chemical structure of the ether moiety and by the degree of substitution, *e.g.*, the number of ether groups per glucose unit, and to a lesser extent by the molecular weight of the polymer and by the fabrication process[58].

Methylcellulose, hydroxypropylcellulose, and hydroxyalkylmethylcellulose, for example, at modest concentrations are soluble in cold water. The incorporation of low levels of hydrophobic modifiers (HM-polymers) on nonionic cellulose ethers results in polymers having highly unusual solution properties. As reported in detail from Landoll[59], this behaviour is thought to be due to interchain association induced by hydrophobic moieties, analogous to the aggregation of low-molecular-weight amphiphatic species into micelles, but the resulting aggregates are three-dimensional polymer networks. As a consequence, he found that the associative tendency (*i.e.* hydrophobic strength) of the modifying group governs both the viscosity and the onset of association (CMC)[a] in solution. Particularly it was found that the concentration of hydrocarbon portion in solution, which depends on the size of the long-chain alkyl group, is closely related to the CMC, suggesting that it represent a critical value for the onset of intermolecular association. Also Winnik et al.[60] demonstrated that the solution properties of HM-cellulose ethers can be explained in terms of interchain polymer associations giving rise to aggregates, which influence the phase behaviour of the polymer solution[61,62].

1.3 Hydroxypropyl cellulose (HPC)

Nearly all polymers, both natural and synthetic, are polydisperse in nature, and cellulose is no exception. Depending on its source and processing, purified cellulose may contain fragments varying in molecular weight from a few thousand to a few million daltons. Usually the molecular size of cellulose and its derivatives is expressed in terms of the degree of polymerization (DP), the average number of anhydroglucose monomer units in polymer chains. Cellulose derivatives, ethers or esters, are formed by appropriate reaction with the three available hydroxyl groups on each anhydroglucose unit; the extent of reaction is described as degree of substitution

---

[a] "The critical aggregation concentration" or CAC is the concentration at which the interaction between surfactant micelles and polymer chains starts. "The critical micellization concentration" or CMC refers to a polymer-free surfactant solution. In our case surfactant and polymer are linked, thus the two terms refer to as the concentration below which virtually no micelles exist and above which almost all additional copolymer goes into the micellar phase[104]

(DS), the average number of the three hydroxyls which are substituted. The substitution of such polymers is expressed in terms of the molar substitution (MS), the average number of moles of reactant combined per mole of monomer units. Whereas the maximum possible DS of a cellulose derivative is three, there is no theoretical limit to the MS[63].

Hydroxypropyl cellulose (HPC), Figure 1.2, is formed from a base-catalyzed reaction of propylene oxide with "alkali cellulose", whereby anionic ring-opening reaction (oligomerization) occurs with scission of the methylene-oxygen bond, the product is etherified by a mixture of "oligo-propylene oxides" having various degrees of polymerization[64]. The properties of HPC are severely influenced by the extent and uniformity of substitution, and much less by the polydispersity of their molecular weight distribution.

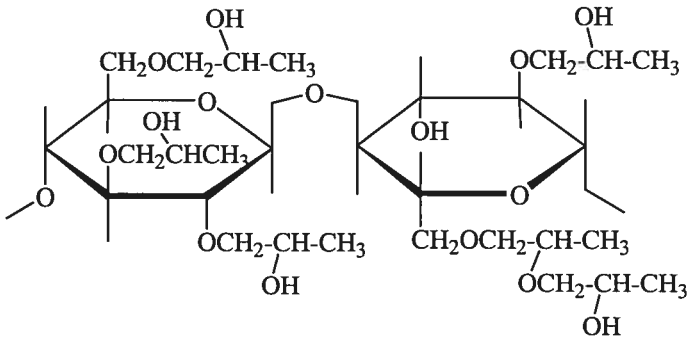

Figure 1.2. Hydroxypropyl cellulose reported as an ideal structure with MS = 3

HPC is a nonionic semiflexible water-soluble polymer. Its characteristics were reported primarily by the Hercules researchers around 1970[65,66]; it is widely used as an excipient in oral solid dosage forms, in which it acts as a disintegrant[67], and as a binder in granulation[68]. Essentially a non-toxic and non-irritant polysaccharide[69], HPC is recognized for its bioadhesive properties, and it is has been shown to promote drug absorption[70].

As most cellulose ethers, HPC precipitates from water upon heating. When an aqueous solution is heated it suddenly becomes cloudy at a characteristic temperature, referred to as the "cloud point" or lower critical solution temperature

(LCST). The phenomenon is reversible: upon cooling, the cloudy suspension becomes clear at the same temperature[61]. It has been demonstrated that even a very small level of substitution of hydrophobic groups affects the solubility of the polymer in water.

For this study we prepare hydrophobically-modified HPC graft copolymers (HPC-*g*-POE_nC_m) of various compositions by attaching hexadecyl or octadecyl residues to the hydrophilic HPC backbone *via* short POE linkers of different lengths (Figure 1.3), and we characterize them from a physicochemical point of view by fluorescence spectroscopy, dynamic light scattering and microcalorimetry techniques.

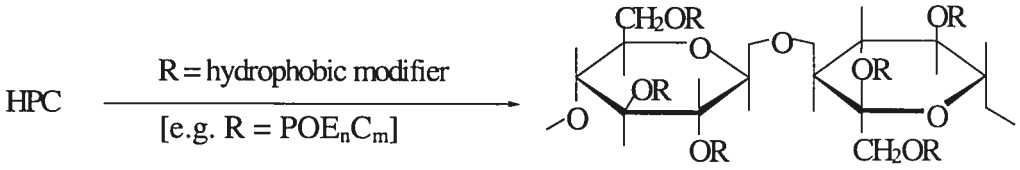

Figure 1.3. Synthetic scheme

1.4 Polyoxyethylene alcohols (Brij®)

Nonionic surfactants containing POE chains as hydrophilic moieties (C_iE_j) are well known and have been widely used for decades. They have found applications in many fields, such as cosmetics, pharmaceuticals, paints, and cleaning agents. Moreover, they are routinely used for the solubilization of membrane proteins[71]. These types of compounds are generally prepared commercially by the condensation of ethylene oxide with fatty alcohols to yield a product in which the hydrophilic portion has a Poisson distribution of chains lengths[72]. These commercial products have been extensively studied[73-75]; they show very rich phase behaviour in aqueous solutions, including phases from isotropic micellar to various ordered liquid crystalline ones. Their general structure is $R(OCH_2CH_2)_nOH$, where R is a long chain alkyl group or mixture of alkyl groups (Figure 1.4).

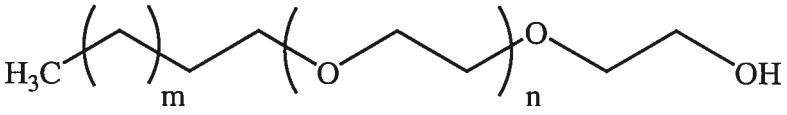

n = 9; m = 13	$POE_{10}C_{16}$ = Brij-56
n = 19; m = 13	$POE_{20}C_{16}$ = Brij-58
n = 19; m = 15	$POE_{20}C_{18}$ = Brij-78

Figure 1.4. Structures and commercial names of Alkylpolyoxyethylenes $POE_{(n+1)}C_{(m+3)}$: Polyoxyethylene(10) cetyl ether (Brij®-56), Polyoxyethylene(20) cetyl ether (Brij®-58) and Polyoxyethylene(20) stearyl ether (Brij®-78).

Like HPC, the poly(ethyleneoxide) type nonionic surfactants possess a concentration- and structure-dependent lower critical solution temperature.

1.5 Cyclosporin A, (CsA), used as drug model

Cyclosporin A (CsA) is a poorly water-soluble nonpolar cyclic peptide (Figure 1.5) comprising 11 aminoacids. It is produced from *Tolypocladium inflatum Gams* (formerly designated as *Trichoderma polysporum*) and other fungi imperfecti[76]. It is used clinically for immunomodulation, such as the prevention of xenograft rejection following transplantation of kidney, liver, bone marrow and pancreas[79-81], and it also applied in the treatment of patients with selected autoimmune diseases[82]. It inhibits the T-cell receptor signal transduction pathway via the formation of cyclosporin A-cyclophilin that inhibits calcineurin (protein phosphatase 2B)[83]. It inhibits nitric oxide synthesis induced by interleukin 1α, lipopolysaccharides and TNFα. and can block cytochrome c release from mitochondria. This drug has a great importance for achieving successful results of organ transplantation, but it must be carefully monitored due to the associated high risk of nephrotoxicity and hepatotoxicity reported in literature[84].

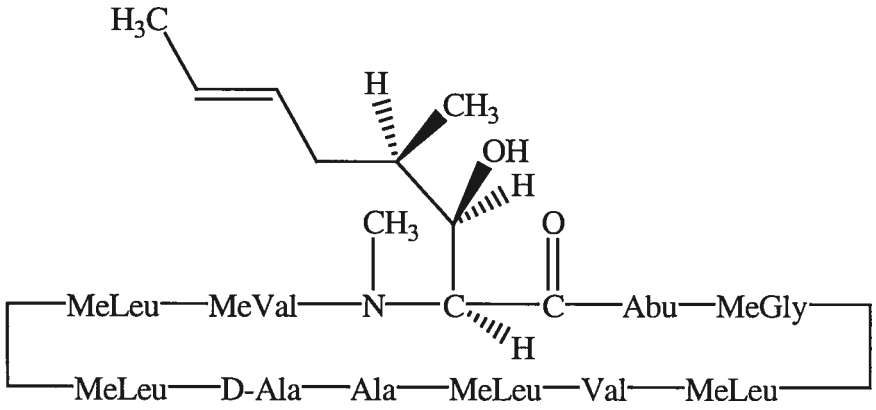

Figure 1.5. Cyclosporin A (CsA); $C_{62}H_{111}N_{11}O_{12}$; MW = 1202.61

CsA is usually administered by the oral route, but it is reported as a typical drug with a non-regular absorption[77,78]. For this reason, this mode of administration presents major problems related to highly variable and incomplete absorption from its conventional oral formulation, leading to tremendous variation in drug pharmacokinetics and, consequently, to an uncertain relation between drug dosage and *in vivo* exposure[85-87]. The absorption of CsA is determined by the biliary flow, by intestinal integrity and motility, and by dietary intake[88-91], and its metabolism is directly related to the cytochrome P-450-III-A in the reticuloendoplasmic system[92]. Due to such characteristics, drug absorption and bioavailability may vary considerably in the same patient and from one patient to another.

It is well known that the absolute bioavailability of CsA is low due to the poor absorption, which is related to the relatively high molecular weight, very high lipophilicity[93] and poor solubility in aqueous fluids[94]; a recent study has demonstrated that low bioavailability is due to the extensive CsA metabolism in the gut wall[95].

1.6 Characterization Methods of HM-Celluloses

1.6.1 Fluorescence spectroscopy

Fluorescence spectroscopy is extensively used in physical chemistry and biochemistry[96]. It is a valuable tool for the investigation of many micellar properties, including micelle formation, micelle-unimer equilibrium, micelle structure as well as chain dynamics, and kinetics of micelle formation and dissociation.

Luminescence is the emission of light from any substance and occurs from electronically excited states. Luminescence is formally divided in two categories, fluorescence and phosphorescence, depending on the nature of the excited state. For fluorescence phenomena, in excited singlet states the electron in the excited orbital is paired (of opposite spin) to the second electron in the ground-state orbital. Consequently, return to the ground state is spin-allowed and occurs rapidly by emission of a photon.

Phosphorescence is emission of light from triplet excited states, in which the electron in the excited orbital has the same spin orientation as the ground-state electron. Transitions to the ground state are forbidden and the emission rates are slow[97].

A Jabłoński diagram, Figure 1.6, illustrates the processes that occur between the absorption and emission of light.

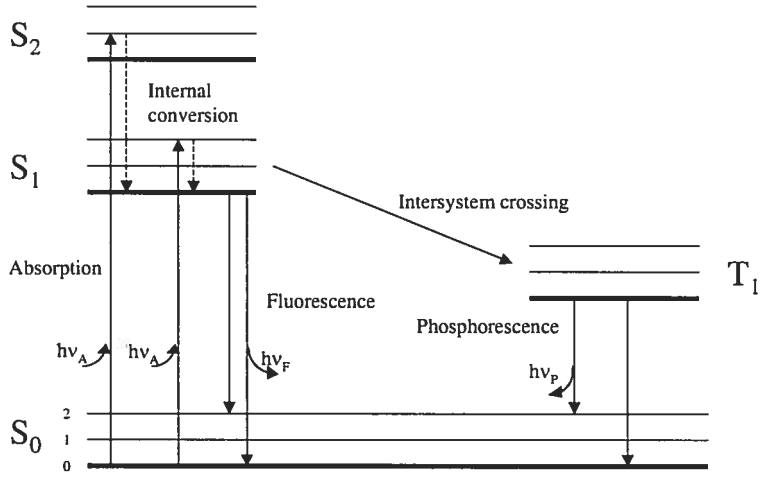

Figure 1.6. One form of Jabłoński diagram

The singlet ground, and first and second electronic states are depicted by S_0, S_1, and S_2, respectively. At each of these electronic energy levels, the fluorophores (fluorescent substances) can exist in a number of vibrational energy levels, denoted by 0, 1, 2, etc.

The transitions between states are depicted as vertical lines to illustrate the instantaneous nature of light absorption or emission. Transitions occur in about 10^{-15} sec, a time too short for significant displacement of nuclei (Frank-Condon principle).

Following light absorption, several processes can occur. A fluorophore is usually excited to some higher vibrational level of either S_1 or S_2. Molecules in condensed phases rapidly relax to the lowest vibrational level of S_1. This process is called internal conversion and generally occurs in 10^{-12} sec or less.

Since fluorescence lifetimes are typically near to 10^{-8} sec, internal conversion is generally complete prior to emission. Hence, fluorescence emission generally results from the thermally equilibrated excited state, that is, the lowest-energy vibrational state S_1.

Return to ground state typically occurs to a higher excited vibrational ground-state level, which then quickly (10^{-12} sec) reaches thermal equilibrium. Molecules in the S_1 state can also undergo a spin conversion to the first triplet state, T_1. Emission from T_1 is termed phosphorescence and is generally shifted to longer wavelengths (lower energy) relative to the fluorescence. Conversion of S_1 to T_1 is called intersystem crossing. Transition from T_1 to the singlet ground state is forbidden, and as a result, rate constant for triplet emission is several orders of magnitude smaller than those for fluorescence[98].

In a fluorescence spectrum excitation *vs* emission (Figure 1.7), the fluorescence intensity is plotted *versus* wavelength (nm).

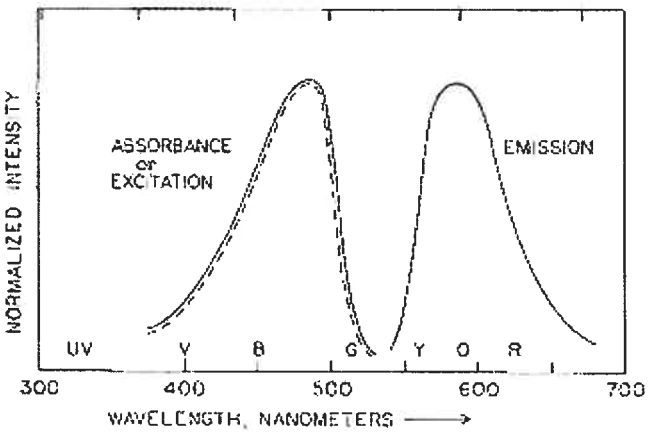

Figure 1.7. Representative excitation and emission spectra

Since the polarity of the environment immediately surrounding a molecule often determines its basic properties, *e.g.* solubility or optical response, it is possible to use fluorescence spectroscopy to detect the formation of the microenvironment within a macroscopically homogeneous solution and to correlate changes in photophysical parameters as a function of various stimuli to structural modifications within the self-assemblies. Fluorescence typically occurs from aromatic molecules; thus, pyrene and other polycyclic aromatic hydrocarbons (PHA) are used extensively for probing local polarity (Figure 1.8).

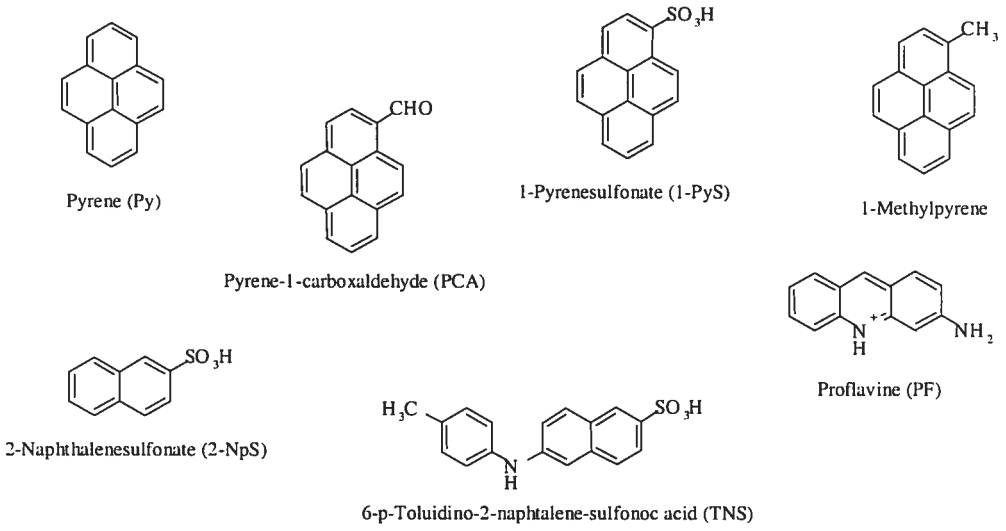

Figure 1.8. Common fluorescent and phosphorescent dyes

Pyrene is by far the most frequently used dye in fluorescence studies, and its spectroscopy is well documented[99]. It has a long singlet lifetime; it readily forms excimers and the vibronic band structure of its emission is sensitive to the environment; it is a strongly hydrophobic probe with low solubility (ca. $3 \cdot 10^{-7}$ M) in water.

Pyrene shows significant fine structure (vibronic bands) in its monomer emission spectrum. In the absence of any solvent interactions with the solute (either individually or collectively), the relative intensities of these vibronic bands in the fluorescence spectrum are governed, as in a UV absorption spectrum, by the relative positions of the potential energy surfaces of the excited singlet states relative to the ground state singlet and by the Franck-Condon principle[100]. At low concentrations (< $1 \cdot 10^{-6}$ M) in homogeneous solution, the ratio of the fluorescence intensity of the highest energy vibration band (I) to the fluorescence intensity of the third highest energy vibrational band (III) undergoes significant perturbation upon going from polar to non-polar solvents[101-104] (Figure 1.9). The I_I peak, which arises from the (0,0) transition from lowest excited electronic state, is a "symmetry-forbidden" transition that can be enhanced by the distortion of the electron cloud. On the other hand, the I_{III} peak is forbidden and thus is relatively solvent-insensitive.

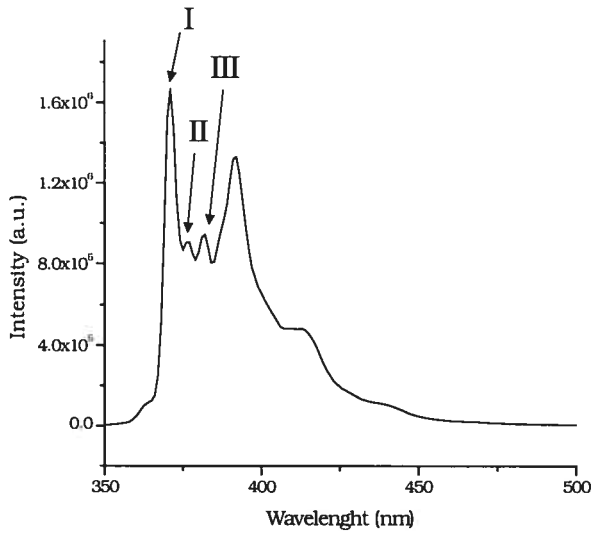

Figure 1.9. Emission spectrum of pyrene in pure water at 25°C

The fluorescence emission probe technique has rather microscopic and dynamic character. It utilizes the information from fluorescence emission spectra of probes incorporated into the polymer. The spectra are sensitive to the change in the environment around the probes; *i.e.*, the change of the conformation of the polymer and the chain dynamics are reflected by the change in spectra. For example, in a plot of copolymer concentration against the I_I/I_{III} ratio from excitation spectra, the phenomenon of micellization is accompanied by an abrupt decrease in I_I/I_{III} (over half a magnitude of concentration). The concentration where this sharp transition occurs is denoted as the critical micelle concentration.

1.6.2 Dynamic Light Scattering (DLS)

Following the pioneering use of lasers and photon beating for the development of dynamic light scattering about thirty years ago, there have been numerous studies using light scattering techniques to investigate liquid dispersions in various research fields. Light scattering is one of the most important ways to characterize new polymeric and colloidal materials[105-108]. Using modern instrumentation, one can readily obtain the weight average molecular weight and radius of gyration from total intensity (static) light scattering, and the hydrodynamic (Stokes) radius from dynamic light scattering that is a non-invasive technique[109] for investigation of dynamic processes by measuring the temporal fluctuations of the scattered light[110]. In general, the scattering and the hydrodynamic behaviour are strongly nonlinear functions of size, due to hydrodynamic interaction if the particles are composed of multiple subunits, and intra-particle interference if they are comparable in size to the wavelength of scattered light[111].

The general equation for the photoelectron count time correlation function is[112]

$$g^{(2)}(\tau) = 1 + \beta\left|g^{(1)}(\tau)\right|^2 \qquad (1)$$

where $g^{(2)}(\tau)$ is a normalized second-order correlation function, β is the optical constant of the instrument, and $g^{(1)}(\tau)$ is a normalized first-order correlation function and is given by formula (2). Γ is a characteristic line width. For spherical particles, Γ is given by a function of the translational diffusion coefficient D_T provided that internal motions are negligible as shown in formulas (3) and (4).

$$g^{(1)}(\tau) = \exp(-\Gamma\tau) \tag{2}$$

$$\Gamma = D_T q^2 \tag{3}$$

$$q = 4\pi n_0 \sin(\theta/2)/\lambda_0 \tag{4}$$

where θ is the scattering angle, λ_0 is the wavelength of the laser, n_0 is the refractive index of the solvent, and q is the magnitude of the scattering vector. In the low concentration region, concentration dependence of the translation diffusion coefficient D_T can be expressed by a linear expression:

$$D_T = D_0(1 + k_d c) \tag{5}$$

where D_0 is the translation diffusion coefficient at infinite dilution, k_d is the diffusion second viral coefficient, and c is the concentration. The hydrodynamic diameter (Stokes diameter) d_h is given by the Stokes-Einstein equation:

$$d_h = k_B T/(3\eta\pi D_0) \tag{6}$$

where k_B is the Boltzman constant, T is the absolute temperature, and η the solvent viscosity.

If there is a distribution in particle size, $g^{(1)}(\tau)$ is expressed by the following equation:

$$g^{(1)}(\tau) = \int G(\Gamma)\exp(-\Gamma\tau)d\Gamma \tag{7}$$

where the G(Γ) is the distribution function of Γ. In the cumulant method, autocorrelation functions are analyzed using an approximate equation

$$g^{(1)}(\tau) = \exp\left[-\bar{\Gamma}\tau + (\mu_2/2)\tau^2 - (\mu_3/3!)\tau^3 + \ldots\right] \tag{8}$$

yielding an average characteristic line width ($\bar{\Gamma}$) and a variance (polydispersity index), $\mu_2/\overline{\Gamma^2}$. In the histogram method, estimation of the size distribution is carried out by a correlation function profile of the histogram analysis software, and eq. (7) is replaced by

$$g^{(1)}(\tau) = \sum G(\Gamma_j)\exp(-\Gamma\tau)\Delta\Gamma \tag{9}$$

and $G(\Gamma_j)$ is determined using the Marquart non-linear least-square routine. $G(\Gamma_j)$, which is a distribution function according to the ratio of light scattering by the particles with Γ, is then converted into the particle size distribution G(*d*) using eqs. (3) and (6). The distribution according to the weight ratio and the number ratio is then determined from G(*d*).

The dynamic light scattering instrument requires a high-power laser, typically an Argon gas laser, a temperature controlled sample cell, a sensitive detector such as a photomultiplier tube, and a time correlator capable of recording intensity (or current) from the photomultipler tube on an extremely short time scale (nanoseconds).

1.6.3 Microcalorimetry

Almost all physical and chemical processes have an associated heat effect, and this can be used as the basis of a number of analytical techniques as well as for the

determination of absolute thermodynamic quantities. Differential scanning calorimetry (DSC) is an experimental technique to measure the heat energy change that takes place in a sample during controlled increase (or decrease) in temperature. At the simplest level, it may be used to determine thermal transition (*e.g.* "melting") temperatures for samples in solution, solid, or mixed phases (*e.g.* suspensions). With a sensitive apparatus and careful experimentation, it may be used to determine absolute thermodynamic data for thermally-induced transitions of various kinds. Formerly this was more the realm of the dedicated specialist, but now with the ready availability of sensitive, stable, user-friendly DSC instruments, microcalorimetry has become part of the standard repertoire of methods available to the biophysical chemist for the study of macromolecular conformation and interactions in solution at reasonable concentrations. The advantages of calorimetric techniques arise because they are based on direct measurements of intrinsic thermal properties of the samples, and are usually non-invasive and require no chemical modifications or extrinsic probes. Furthermore, with careful analysis and interpretation, calorimetric experiments can directly provide fundamental thermodynamic information about the processes involved.

A calorimeter measures the energetics (enthalpy changes) associated with processes that occur, usually, during a linear heating temperature ramp. Measuring the heat flow into (endothermic) or out of (exothermic) a material as it undergoes a phase change yields a plot of temperature-dependent molar heat capacity, Cp.

One of the most fascinating properties exhibited by many water-soluble polymers is reverse temperature-dependent phase behaviour. They form isotropic, one-phase systems in water at or below room temperature, but when heated above a critical temperature (often called the cloud point), they separate into two phases, as indicated visually by a sudden transition from clear solutions to opaque suspensions. The phase transition is reversible: cooling the suspension below the cloud point results in a sudden clarification of the two-phase system[113].

As mentioned earlier, hydroxypropyl cellulose in water exhibits this phenomenon. Functionalization of HPC, *e.g.* by attaching hydrophobic groups, even at a small level of substitution, affects the temperature at which the phase transition occurs[114]. In general, the LCST of HM-HPC is lower than that recorded for a solution of HPC of identical concentration (ca. 45°C for HPC 5.0 mg/mL)[115]; *i.e.* the LCST should decrease with increasing hydrophobicity of the polymer[116,117].

1.6.4 Objectives

Many potent drug candidates fail in preclinical studies because of limited solubility, stability and toxicity. Thus, a number of drug delivery systems have been developed to overcome these transport problems. These include physical aggregates of amphiphilic molecules, such as polymeric micelles.

Major characteristics of these systems are a highly water-soluble core (hydrophobic)-shell (hydrophilic) structure, high carrying capacity of hydrophobic drugs, prolonged storage stability, low viscosity and low interaction with biological components. It is well known that graft copolymers are able to form micelles by themselves in a common good solvent. These phenomena obviously result from the amphiphilic character of the compounds, which contain two groups or sequences greatly different in their solubility behaviour in the same molecule. In aqueous media, formation of hydrophobic regions is due to the hydrophobic interaction between the nonpolar groups, while the shell consists of a dense brush of the hydrophilic segments. Polymeric micelles are an effective vehicle for the solubilization of hydrophobic drugs: the drug can be covalently coupled to the grafted copolymer or physically incorporated into the hydrophobic core of micelles. In contrast to micelles of small surfactant molecules, polymeric micelles are generally more stable and can retain a loaded drug for a longer period of time.

This thesis focuses on the synthesis and physicochemical characterization of new polymeric micelles, which offer potential as carrier systems for hydrophobic drugs and other active molecules. The grafted-polymers were designed to ensure water

solubility and promote hydrophobic associations by a balance between hydrophilic group and hydrophobic moieties, by grafting hydroxypropyl cellulose with hydrophobic hexadecyl and octadecyl residues (HPC-POE_nC_m). Hydroxypropyl cellulose (HPC) was chosen to provide a hydrated steric barrier; POE_nC_m (n = 10/20 and m = 16/18) was chosen as hydrophobic segment, to both maintain the solubility and promote hydrophobic association in water of the novel HM-polymers.

We expected the HM-polymers to form micelles in water solution, exhibiting a strong tendency to self-associate via inter or intrapolymeric interactions of the hydrophobic side chains when the concentration of the amphiphilic graft copolymer is above the critical micelle concentration. We studied aggregation processes of graft-copolymers in dilute solution with fluorescence emission and excitation probe techniques and with microcalorimetry, while the size of these grafted-copolymer micelles was determined by dynamic light scattering.

1.7 References

(1) Lee, V. H. L., *J. Controlled Rel.* **1990**, 13, 213

(2) Lee, V. H. L.; Dodda-Kashi, S.; Grass, G. M.; Rubas, W. In Lee, V. H. L. (Ed.), *Protein and Peptide Drug Delivery*. Marcel Dekker, New York, **1991**, pp. 691

(3) Kim, S. Y.; Shin, I. G.; Lee Y. M. *Biomaterials* **1999**, 20, 1033

(4) Couvreur, P.; Vauthier, C. *J. Controlled Rel.* **1991**, 17, 187

(5) Kreuter, J. *J. Controlled Rel.* **1991**, 16, 169

(6) Weinstein, J. N. In Ostro, M. J. (Ed.), *Liposomes: From Biophysics to Therapeutics*, Marcel Dekker, New York, **1987**, pp. 277

(7) Tardi, P. G.; Boman, N. L.; Cullis, P. R. *J. Drug Targeting* **1986**, 4, 129

(8) Nah, J.-W.; Jeong, Y.-I.; Cho, C.-S. *J. Polym. Sci.: Part B: Polym. Phys.* **1998**, 36, 415

(9) Kreuter, J. *J. Controlled Rel.* **1991**, 16, 169

(10) Seijo, B.; Fattal, E.; Treupel, L.; Couvreur, P. *Int. J. Pharm.* 1990, 62, 1

(11) Peppas, L. *Int. J. Pharm.* **1995**, 116, 1

(12) Cavallaro, G.; Fresta, M.; Giammona, G.; Puglisi, G.; Villari, A. *Int. J. Pharm.* **1994**, 111, 31

(13) Scholz, G.; Iijima, M.; Nagasaki, Y.; Kataoka, K. *Macromolecules* **1995**, 28, 7295

(14) La, S.; Okano, T.; Kataoka, K. *J. Pharm. Sci.* **1996**, 85 (1), 85

(15) Riess, G.; Hurtrez, G.; Bahadur, P. In *Encyclopedia of Polymer Science and Engineering,* 2nd Ed.; Mark, H. F.; Bikales, N. M.; Overberger, C. G.; Menges, G. Eds. Wiley-Interscience: New York, **1985**, 2, 324

(16) La, S. B.; Okano, T.; Kataoka, K. *J. Pharm. Sci.* **1996**, 85 (1), 85

(17) Riess, G.; Hurtrez, G.; Bahadur, P. In *Encyclopedia of Polymer Science and Technology*; Wiley: New York, **1985**

(18) Bader, H.; Ringsdorf, H.; Schmidt, B. *Angew. Makromol. Chem.* **1984**, 123/124, 457

(19) Xu, R.; Winnik, M. A.; Riess, G.; Chu, B.; Croucher, M. D. *Macromolecules* **1992**, 25, 644

(20) Kwon, G.; Naito, M.; Yokoyama, M.; Okano, T.; Sakurai, Y.; Kataoka, K. *Langmuir* **1993**, 9, 945

(21) Gao, Z.; Eisenberg, A. *Macromolecules* **1993**, 26, 7353

(22) Kataoka, K.; Kwon, G. S.; Yokoyama, M.; Okano, T.; Sakurai, Y. *J. Controlled Rel.* **1993**, 24, 119

(23) Zhang, L.; Eisenberg, A. *Science* **1995**, 268, 1728

(24) Nakamura, K.; Endo, R.; Takeda, M. *J. Polym. Sci. Polym. Phys. Ed.* **1976**, 14, 1287

(25) Yokoyama, M.; Inoue, S.; Kataoka, K.; Yui, N.; Okano, T.; Sakurai, Y. *Makromol. Chem.* **1989**, 190, 2041

(26) Nishimura, T.; Sato, Y.; Yokoyama, M.; Okuya, M.; Inoue, S.; Kataoka, K.; Okano, T.; Sakurai, Y. *Makromol. Chem.* **1984**, 185, 2109

(27) Piskin, E.; Kaitian, X.; Denkbas, E. B.; Küçükyavuz, Z. J. *Biomat. Sci. Polym. Ed.* **1995**, 7, 359

(28) Tobio, M.; Gref, R.; Sanchez, A.; Langer, R.; Alonso, M. J. *Pharm. Res.* **1998**, 15, 270

(29) Soma, C. E.; Dubernet, C.; Barratt, G.; Nemati, F.; Appel, M.; Benita, S.; Couvreur, P. *Pharm. Res.* **1999**, 16, 1710

(30) Cammas-Marion, S.; Béar, M.-M.; Harada, A.; Guérin, P.; Kataoka, K. *Makromol. Chem. Phys.* **2000**, 201, 355

(31) Kwon, G. S.; Kataoka, K. *Adv. Drug. Delivery Rev.* **1995**, 16, 295

(32) Trubetskoy, V. S.; Frank-Kamenetsky, M. D.; Whiteman, K. R.; Wolf, G. L.; Torchilin, V. P. *Acad. Radiol.* **1996**, 3, 232

(33) Nagarajan, R.; Barry, M.; Ruckenstein, E. *Langmuir*, **1986**, 2, 210

(34) Moffitt, M.; McMahon, L.; Pessel, V.; Eisenberg, A. *Chem. Mater.* **1995**, 7, 1185

(35) Spatz, J. P.; Roesher, A.; Möller, M. *Adv. Mater.* **1996**, 8, 337

(36) Gast, A. P.; Vinson, P. K.; Cogan-Farinas, K. A. *Macromolecules* **1993**, 26, 1774

(37) Antonietti, M.; Heinz, S.; Schmidt, M.; Rosenauer, C. *Macromolecules* **1994**, 27, 3276

(38) Zhao, J. Q.; Pearce, E. M.; Kwei, T. K.; Jeon, H. S.; Kesani, P. K.; Balsara, N. P. *Macromolecules* **1995**, 28, 1972

(39) Kidchob, T.; Kimura, S.; Imanishi, Y. *J. Controlled Rel.* **1998**, 51, 241

(40) Wang, L-Q.; Tu, K.; Li, Y.; Zhang, J.; Jiang, L.; Zhang, Z. *React. Funct. Polym.* **2002**, 53, 19

(41) Tuzar, Z.; Kratochvil, P. *Adv. Colloid Interf. Sci.* **1976**, 6, 201

(42) Halperin, A.; Tirrell, M.; Lodge, T. P. *Adv. Polym. Sci.* **1992**, 100, 31

(43) Tuzar, Z.; Kratochvil, P. *Surf. Colloids Sci.*; Plenum Press: New York **1993**, 15, 1

(44) Webber, S. E. *J. Phys. Chem. B* **1998**, 102, 2618

(45) Yokoyama, M. *Crit. Rev. Ther. Drug Carrier Syst.* **1992**, 9 (3, 4), 213

(46) Kwon, G. S.; Suwa, S.; Yokoyama, M.; Okano, T.; Sakurai, Y.; Kataoka, K. *J. Controlled Rel.* **1994**, 29, 17

(47) Kwon, G. S.; Naito, M.; Yokoyama, M.; Okano, T.; Sakurai, Y.; Kataoka, K. *Pharm. Res.* **1995**, 12, 192

(48) Cammas, S, Suzuki, K.; Sone, Y.; Sakurai, Y.; Kataoka, K.; Okano, T. *J. Controlles Rel.* **1997**, 48, 157

(49) Chung, J. E.; Yokoyama, M.; Aoyagi, T.; Sakurai, Y.; Okano, T. *J. Controlled Rel.* **1998**, 53 (1-3), 119

(50) Kohori, F.; Sakai, K.; Aoyagi, T.; Yokoyama, M.; Yamato, M.; Sakurai Y.; Okano, T. *Colloids Surf. B: Biointerfaces* **1999**, 16 (1-4), 195

(51) Chung, J. E.; Yokoyama, M.; Okano, T. *J. Controlled Rel.* **2000**, 65, 93

(52) Yokoyama, M.; Okano, T.; Sakurai, Y.; Fukushima, S.; Okamoto, K. Kataoka, K. *J. Drug Targeting* **1999**, 7 (3), 171

(53) Gref, R.; Minamitake, Y.; Peracchia, M. T.; Trubetskoy, V.; Torchilin, V.; Langer, R. *Science*, **1994**, 263, 1600

(54) Kwon, G. S.; Yokoyama, M.; Okano, T.; Sakurai, Y.; Kataoka, K. *Pharm. Res.* **1993**, 11, 970

(55) Kwon, G. S.; Suwa, S.; Yokoyama, M.; Okano, T.; Sakurai, Y.; Kataoka, K. *J. Controlled Rel.* **1994**, 29, 17

(56) Liu, L.; Li, C.; Li, X.; Yuan, Z.; An, Y.; He, B. *J. Appl. Polym. Sci.* **2001**, 80, 1976

(57) Gorshkova, M. Y.; Stotskaya, L. L. Polym. *Adv. Tech.* **1998**, 9, 362

(58) Just, E. K.; Majewicz, T. G.; *Encyclopaedia of Polymer Science and Engineering*, 2nd Ed.; John Wiley: New York, **1985**; Vol. 3, pp 226

(59) Landoll, L. M. *J. Polym. Sci.: Polym. Chem. Ed.*, **1982**, Vol. 20, 443

(60) Winnik, F. M.; Regismond, S. T. A; Goddard, E. D. *Langmuir* **1997**, 13, 111

(61) Winnik, F. M. *Macromolecules* **1987**, 20, 2745

(62) Thuresson, K.; Nilsson, S.; Lindman, B. *Langmuir* **1996**, 12, 2412

(63) Wirick, M. G.; Waldman, M. H. *J. Appl. Polym. Sci.* **1970**, 14, 579

(64) Tezuka, Y.; Imai, K. *Carb. Res.* **1990**, 196, 1

(65) Aqualon; Technical Literature: *Klucel*, Hydroxypropyl cellulose, a nonionic water-soluble polymer: physical and chemical properties, **1987**

(66) Salamon, J. C.; *Polymeric Materials Encyclopedia*, Vol. 5, CRC Press, Boca Raton, **1996**, 3167

(67) Machida, Y.; Nagai, T. *Chem. Pharm. Bull.* **1974**, 22, 2346

(68) Skinner, G. W.; Harcum, W. W.; Barnum, P. E.; Guo, J. H. *Drug Deliv. Ind. Pharm.* **1999**, 25, 1121

(69) Final report on the safety assessment of hydroxyethyl cellulose, hydroxypropyl cellulose, methylcellulose, hydroxypropyl methylcellulose and cellulose gum J. *Am. Coll. Toxicol.* **1986**, 5, 1

(70) Suzuki, Y.; Makino, Y. *J. Controlled Rel.* **1999**, 62, 101

(71) *The Merck Index*; Monography no. 07659

(72) Flory, P. *J. Am. Chem. Soc.* **1940**, 62, 1561

(73) Kushner, L. M.; Hubbard, W. D. *J. Phys. Chem.* **1954**, 58, 1163

(74) Becher, P.; Clifton, N. K. *J. Colloid Sci.* **1959**, 14, 519

(75) Heush, R. *Prog. Colloid Polym. Sci.* **1978**, 65, 186

(76) *The Merck Index*; Monography no. 02781

(77) Klompmaker, I. J. *Ther. Drug Monit.* **1993**, 15, 60

(78) Guo, J.; Ping, Q.; Chen, Y. *Inter. J. Pharm.* **2001**, 216, 17

(79) Matzke, G. R.; Luke, D. R. In Herfindal, E. T.; Gourley, D. R.; Hart, L. L. (Eds.), *Clinical Pharmacy and Therapeutics*. William and Wilkins, Baltimore, **1988**, pp. 229

(80) Lee, M.-K.; Choi, L.; Kim, M.-H.; Kim, C.-K. *Inter. J. Pharm.* **1999**, 191, 87

(81) Mcevoy, G. K. *Cyclosporine.* In Mcevoy G. K.; Litvak, K.; Welsh, O. H. (Eds.), AHFS Drug Information. The American Society of Health System Pharmacists, Inc., Bethesda, **1995**, pp. 2570

(82) Martindale, in: K. Parfitt (Ed.), *The Complete Drug Reference*, 32, Pharmaceutical Press, London, **1999**, pp. 519

(83) Gref. R.; Quellec, P.; Sanchez, A.; Calvo, P.; Dellacherie, E.; Alonso, M. J. *Eur. J. Pharm. Biopharm.* **2001**, 51, 111

(84) Molpeceres, J.; Aberturas, M. R.; Guzman, M. *J. Microencapsulation* **2000**, 17 (5), 599

(85) Kahan, B. D. Pharmacokinetic Profiles of Sandinnum and Neoral. XVth World *Congress of Transplantation Society*, Kyoto, Japan **1994**

(86) Kahan, B. D. *Kidney Inter.* **1993**, 44 (43), 12

(87) Tufverson, G.; Odlind, B.; Sjöberg, A.; Lindberg, A.; Gabrielsson, J.; Lindström, B.; Lithell, H.; Selinus, I.; Tötterman, T.; Wahlberg, J. *Transplant Proc.* **1986**, 18 (5), 16

(88) Grevel, J. *Transplant Proc.* **1986**, 18 (5), 9

(89) Drewe, J.; Berlinger, C.; Kissel, T. Br. *J. Clin. Pharmacol.* **1992**, 33

(90) Reymond, J. P.; Sucker, H.; Vonderscher, *J. Pharm. Res.* **1988**, 5, 677

(91) Wassef, R.; Cohen, Z.; Nordgren, S.; Langer, B. *Kidney Int.* **1985**, 27, 593

(92) McCaughan, G. W.; Bookallilm Sheil, A. *Transplant Proc.* **1994**, 26, 2674

(93) Taylor, N. E.; Mark, A. E.; Vallat, P.; Brunne, R. M.; Testa, B.; Van Gunteren, W. F. *J. Med. Chem.* **1993**, 36, 3752

(94) Ismailos, G.; Reppas, C.; Dressman, J. B.; Macheras, P. *J. Pharm. Pharmacol.* **1991**, 43, 287

(95) Wu, C. Y.; Bennet, L. Z.; Bebert, M. F.; Gupta, S. K.; Rowland, M.; Gomez, D. Y.; Whacher, V. *J. Clin. Pharm. Ther.* **1995**, 58, 492

(96) W. R. G. Baeyens, D. De Keukeleire, K. Korkidis (Eds.), *Luminescence techniques in Chemical and Biochemical Analysis*, M. Dekker, New York, 1991

(97) Atkins, P. W. *Physical Chemistry*, 3rd Ed., **1986**, Oxford University Press

(98) Lakowicz, J. R. *Principles of Fluorescence Spectroscopy*, 2nd Ed, Kluwer Academic, Plenum Publisher, New York

(99) **a**- Winnik F. M. Chem. Rev. **1993**, 93, 587; **b**- Turro, N. J.; Baretz, B. H.; Kuo P.-L. *Macromolecules* **1984**, 17, 1321; **c**- Thomas K. J. *J. Phys. Chem* **1987**, 91, 267; **d**- Fender J. H. *Chem. Rev.* **1987**, 87, 877; **e**- Grieser F.; Drummond C. J. *J. Phys. Chem.* **1988**, 92, 5580; **f**- Ananthapadmanabhan, K. P.; Goddard, E. D.; Turro, N. J.; Kuo P. L. *Langmuir* **1985**, 1, 352; **g**- Winnik, F. M.; Winnik, M. A.; and Tazuke S. *Macromolecules* **1987**, 20, 38; **h**- Riegelman, S.; Aelawala, N. A.; Hrenogg, M. K.; Strait L. A. *J. Colloid Interf. Sci.* **1958**, 13, 208; **i**- Almgren, M.; Grieser, F.; Thomas J. K. *J. Am. Chem. Soc.* **1979**, 101, 279; **j**- Anghel, D. F.; Toca-Herrera, J. L.; Winnik, F. M.; Rettig, W.; Klitzing R. V. *Langmuir* **2002**, 18, 5600; **k**- Karpovich, D. S.; Blanchard G. J. *J. Phys. Chem.* **1995**, 99, 3951; **l**- Winnik, F. M.; Winnik, M. A.; Tazuke S. *J. Phys. Chem.* **1987**, 91, 594; **m**- Turro, N. J.; Chung C-J. *Macromolecules* **1984**, 17, 2123

(100) Kalyanasundaram, K.; Thomas J. K. *J. Am. Chem. Soc.* **1977**, 99, 2039

(101) Reeves, R. L. *J. Am. Chem. Soc.* **1975**, 97, 6019; **1975**, 97, 6025

(102) Shaikh, S.; Asrof Ali, S. K.; Hamad, E. Z.; Al-Nafaa, M.; Al-Jarallah, A.; Abu-Sharkh B. *J. Appl. Polym. Sci.* **1998**, 70, 2499

(103) Thomas, J. K. *Chem. Rev.* **1980**, 80 (4), 283

(104) Munch, M. R.; Gast, A. P. *Macromolecules* **1988**, 21, 1360

(105) Doi, M. *Introduction to Polymer Physics*, 3rd Ed., Oxford University Press, **2001**

(106) Schmitz, K. S. *Introduction to Dynamic Light Scattering by Macromolecules*, Academic Press, Boston, **1990**

(107) Chu, B. *Laser Light Scattering: Basic Principles and Practice*, 2nd Ed., Academic Press, Boston, **1991**

(108) Bee, M. J. Y. *Quasielastic Neutron Scattering: Principles and Applications in Solid State Chemistry, Biology and Materials Science*, Université des Science et des Techniques de Lille Flandres, France, **1988**

(109) Nishiyama, N.; Yokoyama, M.; Aoyagi, T.; Okano, T.; Sakurai, Y. ; Kataoka, K. *Langmuir* **1999**, 15, 377

(110) G. Popescu, A. Dogariu *Applied Optics* **2001**, 24, 40

(111) V. A. Bloomfield *Biopolymers* **2000,** 54, 168

(112) Zhao, C.-L.; Winnik, M. A. *Langmuir* **1990**, 6, 514

(113) Water-Soluble Polymers; J. Glass, Ed.; *Advances in Chemistry Series* **1986**, 213; American Chemical Society : Washington, DC

(114) Winnik, F. M. *Macromolecules* **1987**, 20, 2745

(115) Webowyj, R. S.; Gray, D. G. *Macromolecules* **1984**, 17, 1512

(116) Taylor, L. D.; Cerankowski *J. Polym. Sci., Polym. Chem. Ed.* **1975**, 13, 2551

(117) Webowyj, R. S.; Gray, D. G. *Macromolecules* **1980**,13, 69

CHAPTER 2

2.1 Experimental Section

2.1.1. Materials

Hydroxypropyl cellulose (HPC) with an average molecular weight M_w of ca. 80,000 and a MS of 3.7 was purchased from Aldrich Chemical Co. Polyoxyethylene (10) cetyl ether (POE_{10}-C_{16}; Brij-56®), polyoxyethylene (20) cetyl ether (POE_{20}-C_{16}; Brij-58®) and polyoxyethylene (20) stearyl ether (POE_{20}-C_{18}; Brij-78®) and trimethylamine hydrochloride were purchased from Aldrich Chemical Co. and were dried to constant weight under reduced pressure over P_2O_5 before use. Triethylamine (TEA) and methylene chloride (from Aldrich) were dried over sodium hydride (NaH). *p*-toluenesulfonyl chloride (Aldrich) was used as received. Spectral grade solvents were used. HCl was purchased from Merck KGaA. Sodium hydride (NaH) for the synthesis was purchased as a 60 wt % dispersion in mineral oil (Aldrich). Ion-exchange resins IRA-67 (Aldrich) were regenerated before use with NH_3 2N. Water was distilled and deionized with a Millipore Milli-Q water purification system. Cellulose dialysis tubing (no. 6) from Spectrum Laboratories Inc, had molecular weight cut-off of 8000.

2.1.2 Synthesis of polyoxyethylene (20) cetyl ether tosylate[1,2]

To a solution (cooled in an ice-salt bath) of Brij-58® (6.06 g, 5.40 mmol) in 45 mL of dry CH_2Cl_2 were added Me_3N hydrochloride (266 mg, 2.78 mmol) and TEA (1.5 mL, 1.10 g, 10.83 mmol), under nitrogen. Then a solution of p-toluenesulphonyl chloride (1.59 g, 8.34 mmol) in 15 mL of dry CH_2Cl_2 was added dropwise over a period of 10 min. The solution was stirred at ca. 0 °C overnight. To the reaction mixture was added water (twice, 100 mL), the two phases were separated and to the organic layer was added IRA-67. The slurry was kept (without stirring) at room temperature for 1 h. Filtration and then extraction with water (twice, 50mL) yielded a white product (with a low melting point) (5.5 g; yield = 81%; purity = 85 %). ^{1}H-NMR ($CDCl_3$, δ) 0.9 (t, 3 H), 1.2 (b s, 26 H), 1.6 (quint, 2 H), 2.5 (s, 3 H), 3.4 (t, 2 H), 3.5-3.8 (m, 78 H), 4.1 (t, 2 H), 7.3 (d, 2 H), 7.8 (d, 2 H).

Similarly, tosylation of Brij-56® and Brij-78® was performed.

2.1.3 Synthesis of HPC-g-polyoxyethylene (20) cetyl ether

To prepare the sample with higher Brij-58® content, DMSO was used as solvent reaction. To a solution of HPC (1.02 g) in 30 mL of DMSO, under nitrogen, was added a suspension of NaH (400 mg, wt 60% dispersion in oil, washed twice with dry hexanes) in 30 mL of DMSO. The reaction was stirred mechanically at room temperature for 1 h, and then a solution of Brij-58®-Tos (476 mg, purity 85 %) in 20 mL of DMSO was added drop wise over a period of 15 min.

The reaction was stirred at room temperature for two days. A yellow solution was formed. To the reaction mixture 100 mL of water were added and the excess of base was neutralized with diluted HCl (5 mL, 2 M), and it was extracted with 300 mL of CH_2Cl_2. The two phases were separated and dialysed extensively (Spectra/Por® 6 membranes, MWCO 8.000).

The organic layer was freeze-dried and the crude product (1,24 g) was purified through soxhlet extraction with 500 mL of n-hexanes for 1 day. The final product was dried in vacuo for 24 h to yield 1.06 g of a white amorphous solid (purification yield = 85%). 1.04 g of pure product were solubilized in 50 mL of water; the suspension was then filtered with 0.2 μm Whatman filters. The filtrate was freeze-dried to yield 713 mg of product. By ^{1}H-NMR, the Brij-58® content was found to be 3.9 mol% (all signals were normalized to the HPC anomeric proton signal); (DMSO-d_6, δ) 1.2 (s, 1.0 H), 4.4 (b, 1 H).

Samples with lower Brij-58® content were prepared using tetrahydrofuran (THF) as solvent, and similarly, HPC-g-$POE_{10}C_{16}$, and HPC-g-$POE_{20}C_{18}$ with various molar contents were synthesized using both THF and dimethylformamide (DMF).

^{1}H-NMR spectra were recorded at 400 MHz with a Bruker Avance-400 spectrometer. Spectra were run in chloroform-*d* containing 1 % v/v Me_4Si as internal standard, and in methyl sulfoxide-d_6.

2.1.4 GPC (Gel Permeation Chromatography) analysis

The purity of the HM-polymers and their molecular weight was ascertained by using a refractive index detector for GPC analysis. The GPC instrument was equipped with a Waters 510 HPLC pump, a differential refractometer (Waters 410) and a tunable absorbance detector (Waters 486). The mobile phase was THF, previously degassed. The columns (TSK-GEL Alpha-Guard, 6.0 mm x 4.0 cm, 13 mm; TSK-GEL Alpha-M, 7.8 mm x 30 cm, 13 mm; TSK-GEL Alpha-3000, 7.8 mm x 30 cm, 7 mm) were thermostatted at 40 °C; the flow rate was 0.5 mL/min and the injection volume 30 mL; the UV wavelength was 254 nm and the analysis time was 60 min. The samples were prepared by dissolving HM-polymers, POE_n-C_m and HPC separately at a concentration of 2.5 mg/mL. GPC technique cannot detects little differences of molecular weights: due to the low percentage of substitution, the HM-polymer chromatograms were not expected to change from HPC ones; for the grafted-polymers we observed the same molecular weight of HPC (80.000).

2.1.5 Steady-state fluorescence

Pyrene was used as the hydrophobic fluorescent probe (99 %, Aldrich); it was purified by repeated crystallization from absolute ethanol and subsequent sublimation. Measurements were carried out at room temperature on a Fluorolog-3 Model FL3-11 controlled by DataMax for Windows® software. Emission spectra were recorded at λ_{ex} = 333 nm. Excitation was carried out at λ_{em} = 390 nm. Emission and excitation slits were set at 0.5 mm and 1.0 mm, respectively. From the pyrene excitation spectra, the ratio I_{336} / I_{333} was analysed as a function of concentration of the polymer solution. Values for critical aggregation concentration were determined from the onset of the plot for I_{336} / I_{333} changes (see Results, pag.38).

Stock solutions of HPC-*g*-$POE_{10}C_{16}$, HPC-*g*-$POE_{20}C_{16}$ and HPC-*g*-$POE_{20}C_{18}$, with different MS (Table I, chapter 3), were prepared at room temperature by dissolving the polymer in pyrene-saturated Milli-Q water, previously filtered to remove pyrene microcrystals[3]. It is desirable to achieve molecular solubilization of pyrene in the

given system, i.e. conditions where pyrene groups do not exist as dimers[a] or aggregates[4]. The solutions were allowed to equilibrate for 24 h. HM-polymer solutions of various concentrations were obtained by dilution of the stock solution in pyrene-saturated Milli-Q water. Solutions for the analyses were prepared 24 h before spectroscopic measurements.

The critical aggregation concentration (cac) was obtained from the analysis of the fluorescence excitation spectra of pyrene. With increasing concentration of the HM-polymer, a red shift was observed in the excitation spectrum; that is, the (0,0) band of pyrene shifted from 333 nm (in pure water) to 336 nm in the presence of the polymer (Figure 2.1) at a concentration higher than cac.

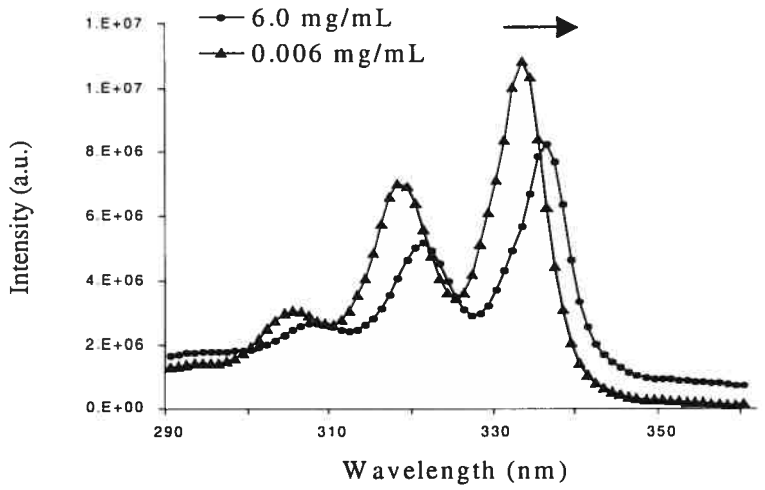

Figure 2.1 Change in the fluorescence characteristic of pyrene as a function of HPC-$POE_{20}C_{18}$ (MS 3.1 mol%) concentration, below (▲) and above (●) the cac.

The ratio I_I/I_{III} of the first (371 nm) and the third (382 nm) vibronic peaks of the fluorescence emission spectrum of micelle-solubilized monomeric pyrene was also determined. It provided an estimate of the polarity sensed by pyrene in its micellar solubilization site (Figure 2.2).

---

[a] An excimer, as defined by Birks, is a dimer which is associated in an electronic excited state and which is dissociated in its ground state. The formation of a pyrene excimer requires the encounter of an electronically excited pyrene with a second pyrene in its ground electronic state. According to this definition, the two pyrenes must be sufficiently far apart when light is absorbed, so that the excitation is localized on one of them; Birks, J. B. *Rep. Prog. Phys.* **1975**, 38, 903

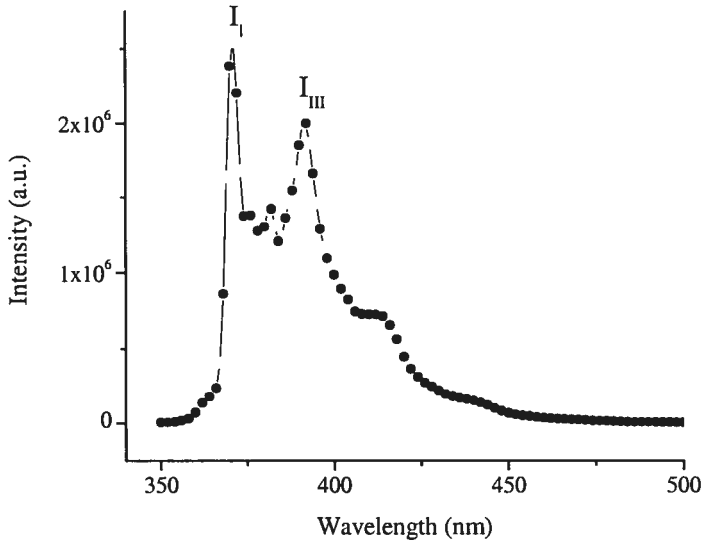

Figure 2.2 Emission spectrum of pyrene in pure water with the labelled peaks I_I and I_{III}.

2.1.6 Dynamic Light Scattering

The hydrodynamic diameter of various HPC-based polymeric micelles in aqueous solution (5 mg/mL) was evaluated by dynamic laser light scattering (DLS) using a Brookhaven system with an uniphase Blue laser at wavelength of 532 nm and a scattering angle of 90 °. All measurements were performed in triplicate at 25 °C; the data presented are the mean ± SD (Standard Deviation).

2.1.7 Microcalorimetry

A VP-differential scanning calorimeter from MicroCal (Northampton, MA) was used. The volume of the cell was about 0.52 mL. Samples for cloud point and microcalorimetric measurements were prepared by dilution of 10 mg of HPC-g-POE_{10}-C_{16}, HPC-*g*-POE_{20}-C_{16} and HPC-*g*-POE_{20}-C_{18}, with different molar substitutions, in 2 mL of Milli-Q water, at room temperature (microcalorimetric technique is very sensitive to sample concentration; after several trials, the sample concentration that gave the best endotherm was 5mg/mL). Samples were degassed and transferred to the sample cell with a calibrated syringe. Milli-Q water was similarly placed in the reference cell. Samples were heated at 30 °C/hr starting from

20 °C up to 80 °C. Four scans were done for each analysis. Baseline subtraction and normalization with respect to the scan rate and mM concentration were performed, yielding the temperature-dependent molar heat capacity, Cp.

The molecular weight of the anhydroglucose unit corresponding to MS = 3.7 is 377[5].

2.2 References

(1) Yoshida, Y.; Sakakura, Y.; Aso, N.; Okada, S.; Tanabe, Y. *Tetrahedron* **1999**, 55, 2183

(2) Cristea, M. *Biomacromolecules* (**2003**), submitted

(3) Winnik, F. M.; Regismond, S. T. A.; Goddard, E. D. *Colloids Surf. A: Physicochem. Eng. Aspects* **1996**, 106, 243

(4) Winnik, F. M. *Chem. Rev.* **1993**, 93, 587

(5) Conio, G.; Bianchi, E.; Cifferi, A.; Tealdi, A,; Aden, M. A. *Macromolecules* **1983**, 16, 1264

CHAPTER 3

3.1 Results and Discussion

Hydrophobically modified (HM)-HPC, namely HPC-*g*-POE_nC_m, was prepared in a two-step reaction from the tosylate of the commercially available POE_nC_m via elimination of the tosyl group by the alkoxide sites formed in the HPC backbone in the presence of a strong base (NaH).

GPC technique is the most widely used method of determining the molecular weight distribution. Separation is accomplished on a column (or a set of columns), packed with gels, which become porous upon swelling that separates the polymer molecules according to size. Separation is based on the hydrodynamic volume of the molecules rather than on the molecular weight. Small molecules are able to diffuse into the pores of the column packing more efficiently, and hence they travel through the columns more slowly: higher molecular weights fractions are thus eluted first.

In a number of molecules the absorption of a photon can be traced to the excitation of the electrons of a small number of atoms. Groups of this kind are called *chromophores* (from the Greek for "color bringer"). Since POE_n-C_m chains have not chromophores, to detect them was necessary to use a universal detector, *e.g.* the refractive index detector; in that way the purity of the HM-polymers, *i.e.* the absence of POE_n-C_m residue, was demonstrated.

Solvent choice was based on the Hydroxypropyl cellulose properties; in fact it is soluble in several organic solvents (*e.g.* THF) as well as in water. For each HM-polymer, as well as for HPC and POE_n-C_m series, we run experiment twice discovering a narrow distribution for HPC samples and a similar behaviour for HM-polymers. As we said earlier GPC technique cannot detects small differences of molecular weights, thus for the grafted-polymers we observed the same molecular weight of HPC. In all cases reproducible traces were obtained with THF solvent (traces not shown).

^{1}H-NMR spectra were used both to ascertain linking of Brij® to the polymer backbone and for a quantitative determination of the level of its incorporation on the

polymer. Signals due exclusively to either the resonance of Brij® aliphatic protons or to the HPC anomeric proton were identified[1,2], as illustrated in Figure 3.1. The singlet at ca. 1.2 ppm was attributed to the resonance of the aliphatic protons of the Brij® chain, while the broad signal at 4.5 ppm was assigned to the resonance of the HPC anomeric proton.

MS (molar substitution) is defined as the average number of moles of reactant combined per mole of sugar unit[1,3]. The MS of HPC-g-POE_nC_m was calculated using the formula[4]:

$$I_a / 2(m-3)H \times 100$$

where I_a is the average integral of the aliphatic protons [$(CH_2)_{m-3}$] of the POE_nC_m chain and the theoretic number of protons assigned to that signal (*i.e.* 26 for $POE_{10}C_{16}$ and $POE_{20}C_{16}$; 28 for $POE_{20}C_{18}$) (see spectrum 9 for more details).

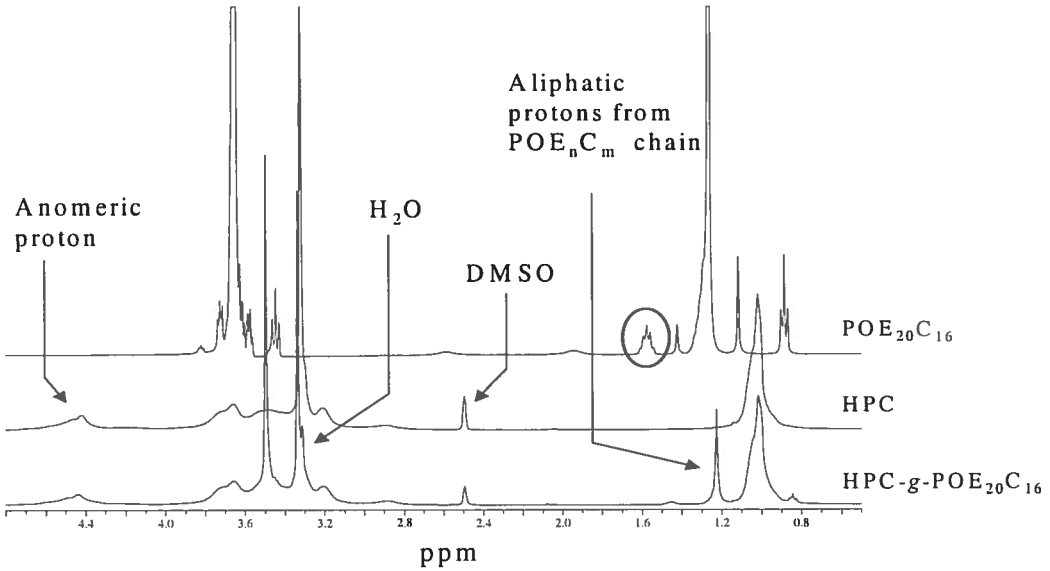

Figure 3.1. ^{1}H-NMR spectra of Brij-58®, HPC and HPC-$POE_{20}C_{16}$; the former in $CDCl_3$ and the others in DMSO-d_6.

The synthesized HM-polymers and their respective MS degrees are summarized in Table I.

3.1.1 Fluorescence

Fluorometric measurement with a hydrophobic probe is a powerful method to investigate organized assemblies, since fluorescence of dyes, solubilized into the hydrophobic region reflect sensitively the change in the microenvironment[5-8]. The relatively long lifetime of the pyrene excited single state and its strong affinity for hydrophobic regions has prompted its use as a fluorescent probe for the hydrophobic regions of micelles and other biological macromolecules[9-11]; its partitioning in the hydrophobic microdomain causes changes in photophysical properties.

Usually, these changes accompany the transfer of pyrene molecules from a water environment to the hydrophobic micellar cores and thus they provide information on the location of the pyrene probe in the system.

A probe molecule may be adsorbed to the surface of the micelle or, alternatively, it may be solubilized in the hydrocarbon core. Several studies provide useful information on the location of the dye in the micelle and, one of these makes use of the effect of the environment on the spectral properties of probe molecules. Pyrene itself shows a fluorescence with distinct vibrational structure (Figure 3.2), thus the I/III band ratio can be used to gain some measure of the polarity of the probe environment into these micelles. Due to changes in the local polarity, the vibrational structure of the pyrene monomer emission spectrum changes upon the formation of polymeric micelles, this is known as the Ham effect[12]

The same phenomenon can be studied with fluorescence excitation spectra, in fact increasing polymer concentration in an aqueous solution of pyrene, a shift of the band from 333 nm to 336 nm can be observed (Figure 3.3).

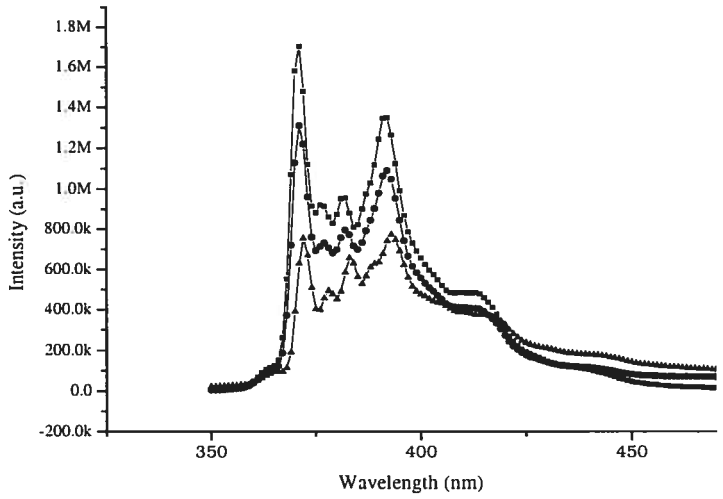

Figure 3.2 Emission spectra of pyrene in aqueous solutions of HPC-*g*-POE_{20}-C_{16} (ca. 3.9%) at different polymer concentrations [pyrene in pure water (■), HM-polymer 0.006mg/mL (●), HM-polymer 0.6 mg/mL (▲)]. λ_{ex}= 333nm

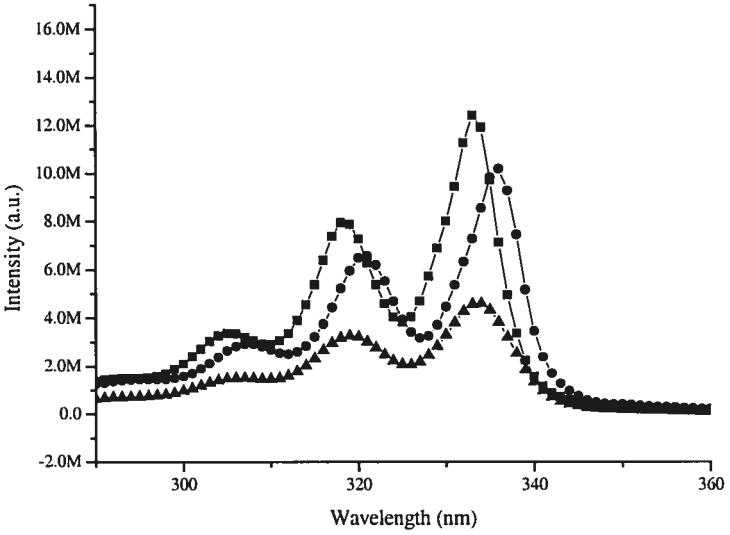

Figure 3.3 Excitation spectra of pyrene in aqueous solutions of HPC-*g*-POE_{20}-C_{18} (ca. 3.1%) at different polymer concentrations [HM-polymer 0.006 mg/mL (■), HM-polymer 0.6mg/mL (●), HM-polymer 0.06 mg/mL (▲)]. λ_{em}= 390nm

Plotting the I/III band intensity ratio of pyrene monomer versus the dependence of the logarithm of the concentration, it was found that, below the critical aggregation concentration, there are no micelles present in the system and the pyrene fluorescence

spectrum corresponds to that in pure water, with an I_I/I_{III} ratio of about 1.7 - 1.8. As the polymer concentration increases above the cac, pyrene is progressively solubilized into the hydrophobic interior, as indicated by the drastically decreased I_I/I_{III} ratio in the intermediate region of polymer concentration. The I_I/I_{III} values of about 1.20 for the higher concentration regions of the polymer indicate that the location of the pyrene probe is primarily in the nonpolar environment of the micellar core.

Different methods can be used to determine the CAC values[13]: the true onset of aggregation is a rather delicate problem because the change in fluorescence signal can be influenced not only by polymer association but also by the partition of the fluorescence probe between the aqueous and the hydrophobic phases[14], since the micelle is characterized by regions of different polarity.

One approach is to fit the I_{336}/ I_{333} ratio (or the I_I/I_{III} ratio) versus log C plot to a sigmoidal curve; CAC was taken as the intersection of the horizontal tangent through the points at the lowest polymer concentration with the tangent to the fitting curve at the inflection point (dashed line in Figures 3.4 and 3.5).

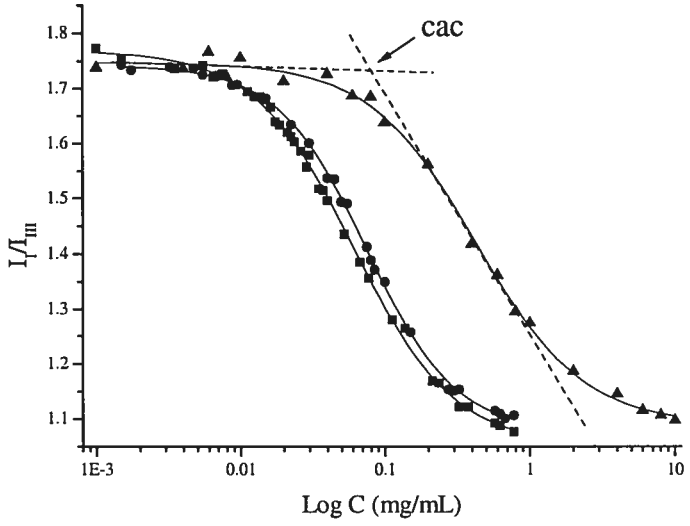

Figure 3.4. Plots of pyrene intensity ratio I_I/I_{III} as a function of HM-polymers concentration. (■) HPC-$POE_{10}C_{16}$ 4.7 mol%, (●) HPC-$POE_{10}C_{16}$ 5.4 mol%, (▲) HPC-$POE_{10}C_{16}$ 0.9 mol%; for all cases, as the polymer concentration increases above the cac, the I_I/I_{III} ratio decreases.

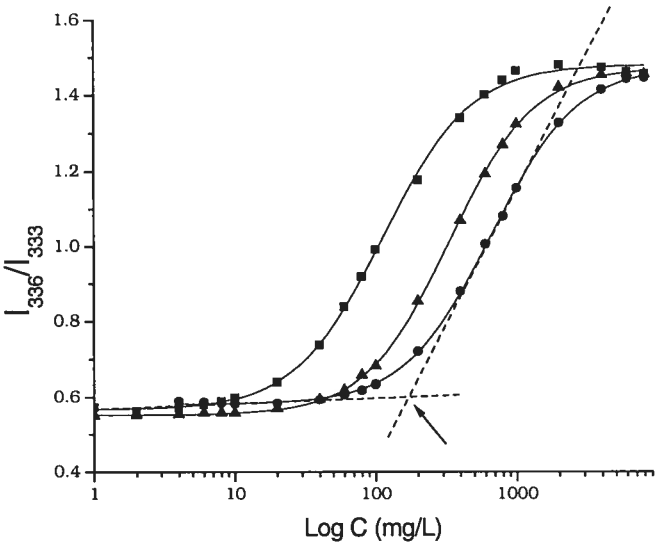

Figure 3.5. Plots of pyrene intensity ratio I_{336}/I_{333} as a function of HM-polymers concentration. (■) HPC-$POE_{20}C_{18}$ 3.1 mol%, (●) HPC-$POE_{20}C_{18}$ 1.1 mol%, (▲) HPC-$POE_{20}C_{16}$ 1.1 mol%; the arrow shows the CAC value for HPC-$POE_{20}C_{18}$ 1.1 mol% sample.

Polymer composition	MS (mol %) [b]	cac Polymer concentration (mg/L) [c]			Particles diameter (nm)
		Onset	Middle point	Offset	
HPC-*g*-POE_{10}-C_{16}	0.9	94 ± 2.8	428 ± 9.2	1850 ± 3.5	85 ± 2
HPC-*g*-POE_{10}-C_{16}	4.7	16 ± 0.1	78 ± 0.7	328 ± 3.5	80 ± 1
HPC-*g*-POE_{10}-C_{16}	5.4	22 ± 0.7	81 ± 4.2	300 ± 6.4	66 ± 2
HPC-*g*-POE_{20}-C_{16}	1.1	82 ± 2.1	334 ± 2.1	1313 ± 17.7	90 ± 0.5
HPC-*g*-POE_{20}-C_{16}	3.9	18 ± 0.3	79 ± 0.4	324 ± 7.1	78 ± 0.8
HPC-*g*-POE_{20}-C_{18}	1.1	153 ± 2.1	657 ± 0.1	2618 ± 35.4	85 ± 0.8
HPC-*g*-POE_{20}-C_{18}	3.1	27 ± 0.1	113 ± 5.7	502 ± 7.8	83 ± 2
POE_{10}-C_{16}	100	5.1 ± 1.0	-	-	-
POE_{20}-C_{16}	100	5.0 ± 0.6	-	-	-
POE_{20}-C_{18}	100	4.1 ± 0.6	-	-	-

Table I. CAC values and particle mean diameters of aqueous solution of HPC-POE_nC_m; [b] Determined by ^{1}H-NMR measurement in DMSO-d_6;[c] Determined by change in I_{336} nm /I_{333} nm ratio of pyrene fluorescence with log polymer concentration at 25 °C.

The CAC values (Table I) range from 16 to 150 mg/L. For the three series of HM-polymers, indicates that the increase in the HPC molar substitution is accompanied by a decrease in the CAC value. For example, HPC-*g*-$POE_{10}C_{16}$ with a molar substitution of 5.4 mol% shows a CAC of 22mg/L, while that of HPC-*g*-$POE_{10}C_{16}$ 0.9 mol% is 94 mg/L; HPC-*g*-$POE_{20}C_{16}$ 1.1% has a CAC of 82 mg/L while the one with 3.9% has CAC of 18 mg/L; finally, HPC-*g*-$POE_{20}C_{18}$ behave in the same way. That agrees with the theory that wants a lower CAC value as the hydrophobic moiety enhances[15-17].

Furthermore, in alkylpoly(ethylenoxide) micelles the position of the probe is probably more widely distributed, ranging from the α-CH_2-group of the hydrocarbon core to quite peripheral positions in the $-(OCH_2CH_2)_n$-OH mantle[18]; that could explain why for HPC-*g*-$POE_{10}C_{16}$ (0.9 mol%) and HPC-*g*-$POE_{20}C_{16}$ (1.1 mol%) we found almost the same CAC value 94 mg/L and 82 mg/L respectively, meaning that the POE chain length has not significant affect on the partitioning of pyrene in the micelles.

On the other hand, the major contributing factors to the depression of the CAC may be (1) the hydrophobic interaction between the alkyl chains, which is the main driving force; (2) specific interactions and attractions between the HM-polymer segments[19]: in fact the associative tendency (i.e. hydrophobic strength) governs also the ability to form network structures. As a result, is very difficult to explain such little differences in the HM-polymer CAC trend, and more studies should be performed.

To better illustrate the hydrophobicity trend, the dependence of I_{336}/I_{333} ratio was plotted against the moles of Brij® per litre of aqueous solution of HM-polymers, and corresponding CAC values were determined with the method previously described (Figure 3.6 and Table II).

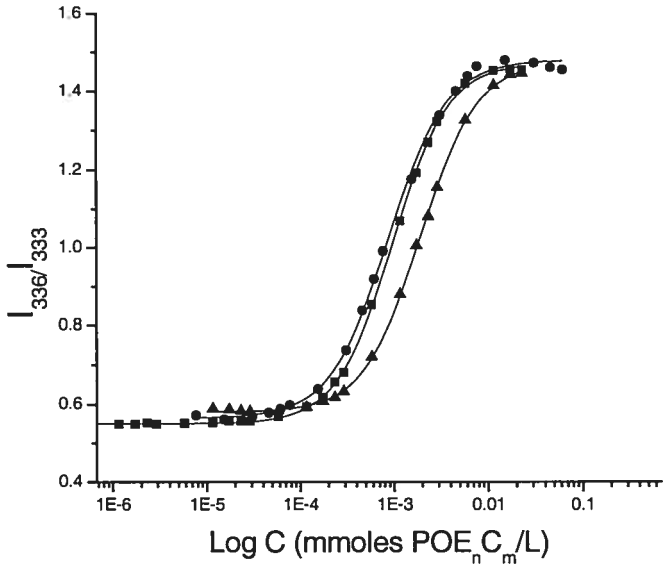

Figure 3.6. Plots of pyrene intensity ratio I_{336}/I_{333} as a function of mmol POE_nC_m per litre of solution. (●) HPC-$POE_{20}C_{18}$ 3.1 mol%, (▲) HPC-$POE_{20}C_{18}$ 1.1 mol%, (■) HPC-$POE_{20}C_{16}$ 1.1 mol%.

Polymer composition	MS (mol%)	Onset conc. (mmoles of POE_nC_m/L)
HPC-*g*-POE_{10}-C_{16}	0.9	0.24 ± 0.1
HPC-*g*-POE_{10}-C_{16}	4.7	0.21 ± 0.0
HPC-*g*-POE_{10}-C_{16}	5.4	0.31 ± 0.0
HPC-*g*-POE_{20}-C_{16}	1.1	0.25 ± 0.1
HPC-*g*-POE_{20}-C_{16}	3.9	0.18 ± 0.0
HPC-*g*-POE_{20}-C_{18}	1.1	0.47 ± 0.1
HPC-*g*-POE_{20}-C_{18}	3.1	0.21 ± 0.1

Table II. Hydrophobic content in HM-Polymers expressed as mmoles of POE_nC_m per litre of solution

We highlight an anomalous behaviour between HPC-*g*-POE_{10}-C_{16}, HPC-*g*-POE_{20}-C_{16} and HPC-*g*-POE_{20}-C_{18} series: in the first case the trend is opposite and the CAC value increases as the hydrophobic percentage increases.

It can be concluded that, in general, the partitioning of pyrene in the micelle is determined mainly by the molar substitution of the HM-polymer.

3.1.2 Dynamic Light Scattering

Compared with other type of carrier systems, the polymeric micelles possess several benefits[20,21] including their size, which is approximately from 20 to 100 nm. This range of diameter is smaller than typical diameter of liposomes and nanospheres. The smaller carrier systems are expected to show the higher vascular permeability at target sites by a diffusion mechanism. Furthermore, they have the potential to decrease RES (reticuloendothelial system) uptake because the diameter ranges (less than ca. 100) are considered small enough to evade non-specific capture by RES. If they are administered intravenously, their size may be advantageous for extravasations, which should be an essential process for the carrier to reach the target located outside of the capillaries.

The size distribution of HPC-POE_nC_m micelles measured by DLS showed a narrow monodisperse size distribution with the average diameter less than 90 nm, Table I.

3.1.3 Microcalorimetry

Lower critical solution temperatures (LCSTs) are found in many polymer solutions characterized by strong hydrogen bonds[22]. The formation of hydrogen bonds between solutes and solvents lowers the free energy of solution; however, the specific molecular orientations required by these bonds leads to negative entropy changes and positive contributions to free energy. This phenomenon is particularly important in aqueous media where a further negative entropy change is contributed by the hydrophobic effect. When the temperature of a HM-polymer solution is raised above the LCST, negative entropy dominates the otherwise exothermic enthalpy of the hydrogen bonds formed between the polar groups and water molecules, i.e. the initial driving force for dissolution. Thermal destruction of the specific water orientations around hydrophobic polymer regions facilitates polymer-polymer associations by hydrophobic interactions, resulting in polymer precipitation[23]. Copolymers exhibiting LCST behaviour have been investigated for applications such as controlled drug

delivery and solute separation. An important and useful feature of thermosensitive polymers is the possibility of controlling their LCST by various means, in particular by varying the copolymer composition.

HPC is a well-known water-soluble polymer, showing reversible hydration-dehydration changes in response to a small solution temperature change. The LCST of HPC in water is known to be ca. 47°C. Several hypotheses to explain HPC behaviour in aqueous solution have been suggested[24-26].

However, the mechanism of the temperature-induced phase separation and the influence on the LCST are not fully understood. In general, the incorporation of hydrophobic elements lowers the cloud point as would be expected from its decreasing hydrophilic character[27].

The specific role of molar substitution was examined (Figure 3.7). The temperatures at the maxima of the DSC endotherm were referred to as the LSCT's of the HM-polymers. The change in LCST was found to be proportional to the MS content. The increase in LCST was the largest for the HPC-$POE_{20}C_{16}$ 3.9 mol% followed by the HPC-$POE_{20}C_{18}$ 3.1 mol%, while the highest hydrophobic substitution in HPC-$POE_{10}C_{16}$ 5.4 mol% caused a decrease in the LCST (Table III).

It is generally accepted that LCST behaviour is caused by a critical hydrophilic/hydrophobic balance of polymer side groups. For HPC-POE_nC_m the HPC is the hydrophilic element and POE_nC_m are the hydrophobic groups. At low temperature the strong H-bonding between the hydrophilic groups and water outweighs the unfavourable free energy related to the structure of water around hydrophobic groups, leading to good solubility of polymer in water. At increasing temperatures, H-bonding weakens, while hydrophobic interaction between hydrophobic side group increase. Above the LCST, interactions between hydrophobic groups become dominant, leading to an entropy-driven polymer collapse and phase separation[28]. Our results agree with this theory only for the $POE_{10}C_{16}$ kind of hydrophobic element, in fact $POE_{10}C_{16}$ 0.9 % and $POE_{10}C_{16}$ 5.4 % have 46.7 °C and 46.1 °C of cloud point, respectively (Figure 3.7). In the other two cases the HM-polymers with the highest molar substitution show an opposite trend and for HPC-$POE_{20}C_{16}$ 3.9 mol% and HPC-$POE_{20}C_{18}$ 3.1 mol% the LCST are higher

than that of HPC, 51.9 °C and 49.3 °C respectively. A possible explanation for this anomaly could come if we consider that the phase separation is driven by a reduced amount of structured water around hydrophobic groups with increasing temperature, which results in increased hydrophobic interactions between polymers[29]. $POE_{20}C_{16}$ and $POE_{20}C_{18}$ have a hydrophilic chain length double than that of $POE_{10}C_{16}$ thus, it is possible that strong H-bonding between that chains and water are predominant with respect to the hydrophobic intermolecular interactions leading an increase LCST; but, as we said before, the LCST behaviour is caused by a critical hydrophilic/hydrophobic balance of polymer side groups.

Furthermore, the heat of transition (ΔH) differs significantly from one sample to another: an increase in substitution results in a decrease of heat flows and a broadening of the endotherm. Some authors attribute the ΔH value to the breakage of hydrogen bonds between water molecules and polymer's functional groups[30]. Some others attribute the heat of transition to the destruction of water-water hydrogen bonds in the hydrophobic hydration shell[22,31]. At the moment we have no good explanation for this behaviour and further studies are in progress.

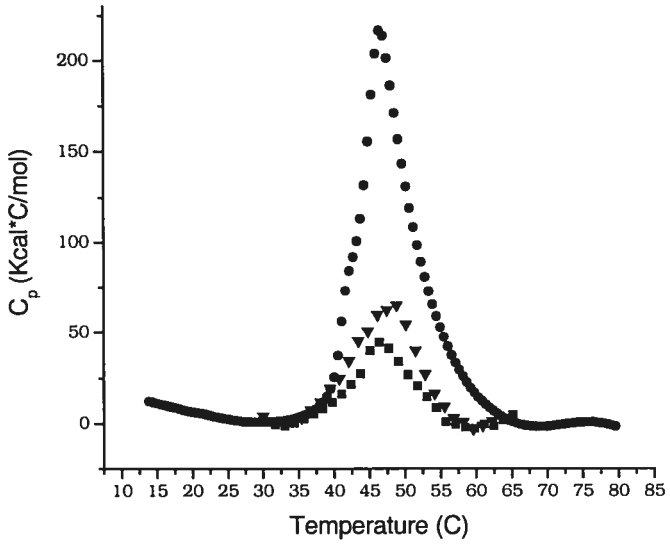

Figure 3.7. Microcalorimetric endotherm of aqueous solution of HPC-$POE_{10}C_{16}$ with different MS. (●) 0.9 mol%, (▼) 4.7 mol%, (■) 5.4 mol%. 30 °C/hr from 20 °C to 80 °C.

Polymer composition	MS (mol %)	cloud point (°C)[a]	ΔH (Kcal/mol)[a]
HPC	0	47.9 ± 0.1	2.1 ± 0.2
HPC-*g*-POE_{10}-C_{16}	0.9	46.7 ± 0.1	1.9 ± 0.1
HPC-*g*-POE_{10}-C_{16}	4.7	46.6 ± 0.1	0.73 ± 0.1
HPC-*g*-POE_{10}-C_{16}	5.4	46.1 ± 0.1	0.41 ± 0.1
HPC-*g*-POE_{20}-C_{16}	1.1	47.3 ± 0.1	2.4 ± 0.0
HPC-*g*-POE_{20}-C_{16}	3.9	51.9 ± 0.3	0.67 ± 0.0
HPC-*g*-POE_{20}-C_{18}	1.1	48.0 ± 0.1	3.5 ± 0.0
HPC-*g*-POE_{20}-C_{18}	3.1	49.3 ± 0.1	0.46 ± 0.1

Table III. Cloud points and heats of transition (ΔH) of aqueous solutions of HM-polymers; [a]experiment performed in triplicate and then calculated the SD.

3.2 References

(1) Tezuka, Y.; Imai, K. *Carb. Res.* **1990**, 196, 1

(2) Fernandez, M. A.; Granados, A. M.; El Seoud, O. A; de Rossi, R. H. *Langmuir* **2002**, 18, 8786

(3) Wirick, M. G.; Waldman, M. H. *J. Appl. Polym. Sci* **1970**, 14, 579

(4) Dubé, D.; Francis, M.; Leroux, J.-C.; Winnik, F. M. *Bioconjugate Chem.* **2002**, 13, 685

(5) Dong, D. C.; Winnik, M. A. *Photochem. Photobiol.* **1982**, 35, 17

(6) Morishima, Y. *Trip* **1994**, 2 (1), 31

(7) Dowling. K. C.; Thomas, J. K. *Macromolecules* **1990**, 23, 1059

(8) Ikemi, M.; Odagiri, N.; Tanaka, S.; Shinohara, I.; Chiba, A. *Macromolecules* **1981**, 14, 34-39; *Macromolecules* **1982**, 15, 281

(9) Morishima, Y. *Prog. Polym. Sci.* **1990**, 15, 949

(10) Kakyanasundaram, K.; Grätzel, M.; Thomas, J. K. *J. Am. Chem. Soc.* **1975**, 97 (14), 3915

(11) Winnik, F. M.; Regismond, S. T. A. *Polymer-Surfactant Systems of the Surfactant Science-Series*, Vol. 77, New York, **1998**, Ed. by Jan C. T. Kwak

(12) Nagasaki, Y.; Okada, T.; Scholz, C.; Iijima, M.; Kato, M.; Kataoka, K. *Macromolecules* **1998**, 31, 1473

(13) Astafieva, I.; Zhong, X. F.; Eisenberg, A. *Macromolecules* **1993**, 26, 7339

(14) Wilhelm, M; Zhao, C.-L.; Wang, J.; Xu, R.; Winnik, M. A.; Mura, J.-L.; Reiss, G.; Croucher, M. D. *Macromolecules* **1991**, 24, 1033

(15) Landoll, L. M. *J. Polym. Sci.: Polym. Chem. Ed.*, **1982**, Vol. 20, 443

(16) Winnik, F. M. *Macromolecules* **1987**, 20, 2745

(17) Thuresson, K.; Nilsson, S.; Lindman, B. *Langmuir* **1996**, 12, 2412

(18) Grieser F.; Drummond C. J. *J. Phys. Chem.* **1988**, 92, 5580

(19) Wang, Y; Han, B; Yan, H. *Langmuir* **1997**, 13, 3119

(20) Chi, S.-C.; Yeom, D.-I.; Kim, S.-C.; Park, E.-S. *Arch.Pharm. Res.* **2003**, 26 (2), 173

(21) Yokoyama, M. *Crit. Rev. Ther. Drug Carrier Syst.* **1992**, 9 (3,4), 213

(22) Schild, H. G.; Tirrell, D. A. *J. Phys. Chem.* **1990**, 94, 4352

(23) Chung, J. E.; Yokoyama, M.; Aoyagi, Y.; Sakurai, Y.; Okano, T. *J. Control. Rel.* **1998**, 53, 119

(24) Drummond, C. J.; Albers, S.; Furlong, D. N.; *Colloids Surf.* **1992**, 62, 75

(25) Lu, X.; Hu, Z.; Schwartz, J. *Macromolecules* **2002**, 35, 9164

(26) Kug, E.D. *J. Polym. Sci., Part C* **1971**, 36, 491

(27) Taylor, L. D.; Cerankowski; L. D. *J. Polym. Sci., Polym. Chem. Ed.* **1975**, 13, 2551

(28) Feil, H.; Bae, Y. H.; Feijen, J.; kim, S. W. *Macromolecules* **1993**, 26, 2496

(29) Bae, Y. H.; Okano, T.; Kim, S. W. *J. Polym. Sci., Polym. Phys. Ed.* **1990**, 28, 923

(30) Otake, K.; Inomata, h.; Konno, M.; Saito, S. *Macromolecules* **1990**, 23, 283

(31) Schild, H. G.; Muthkumar, M.; Tirrell, D. A. *Macromolecules* **1991**, 24, 948

CHAPTER 4

4.1 Conclusions

In recent years, there have been growing interests in macromolecular micelles in aqueous media. This is not only because of their photochemical and biological relevance but also because of their potential importance in application in drugs, coatings, paints, oil recovery, and flocculation of water waste and personal care goods.

As described in the introduction, polymeric micelles have advantageous features summarized as a) highly hydrated polymeric micelle outer shell that can inhibit intermicellar aggregation of the hydrophobic inner cores; consequently, they maintain their water solubility irrespective of the high content of the hydrophobic drug inside the inner cores; b) polymeric micelle size is usually less than 100 nm, which prevents non-selective scavenging from the RES; c) stability and slower dissociation; d) protection of the incorporated drug from the aggressive conditions present in the gastrointestinal tract.

This work mainly featured the modification of hydroxypropyl cellulose with long-chains POE_nC_m. The balance between the stability and the solubilizing power of the micelle is quite important; thus, a rationale project was required for the structural design of the inner core segment in terms of length, chain mobility, the nature of cohesive forces and biocompatibility

The project resulted in a promising new class of synthetic nonionic water-soluble polymers with a suitable hydrophilic/hydrophobic balance for the formation of micelle structures in water. These grafted copolymers are typically several tens of nanometres in diameter with a relatively narrow size distribution, and are therefore similar in size to viruses, lipoproteins, and other naturally occurring transport systems. HM-polymers have been characterized from a chemical and physical point of view by ^{1}H-NMR, GPC, fluorescence spectroscopy and DSC techniques. The molar substitution was estimated to be in the range of 0.9 % - 5.4 %.

The synthesized HM-polymers exhibit a strong tendency to self-associate via inter or intrapolymeric interactions of the hydrophobic side chains: the cohesive interactions for micelle formation include hydrophobic interaction, ionic interaction, and

hydrogen bonding. Exploiting emission and excitation spectra of pyrene, micelle formation was followed and the critical aggregation concentrations were determined to be in the range of 16 – 150 mg/L; it was found that they are highly dependent on the increased hydrophobic character.We confirmed that the critical micelle concentration increases as the relative length of the less soluble block decreases, and as the solubility of the head group increases.

Polymeric micelles are expected to retain water solubility even when diluted at body temperature: microcalorimetry has been successfully applied to study the LCST of the polymers in aqueous media proving their solubility at 37 °C. The experimental results indicate that temperature-induced phase separation of solutions of LCST polymers are mainly driven by increased interactions between hydrophobic moieties on the polymers, caused likely by a reduced structuring of water around hydrophobic polymer side groups (decreased stabilization of hydrophobic groups in water) with increasing temperature. Changes in LCST caused by the incorporation of long-chain POE_nC_m are due to changes in overall hydrophilicity of the polymer; in fact the HPC functionalization with a larger fraction of hydrophobic moieties enhances association in water leading to a cloud point temperature decrease.

The mean diameter of polymeric micelles was found to be less than 90 nm, thus stable aqueous dispersions of these HM-polymers presents potential for a versatile administration route.

This thesis focused on the chemical and physical characterization of the HM-polymers. In parallel to this, another study was performed to exploit the solubilizing potential of hydroxypropylcellulose-*g*-polyoxyethylene alkyl ether polymeric micelles towards poorly water soluble-drugs, and improve their oral bioavailability: Cyclosporin A (CsA), a poorly water immunosuppressant, was selected as model drug.

CsA loading into HPC-*g*-$(POE)_nC_m$ polymeric micelles was significantly larger than in unmodified HPC. It increased with increasing number of POE_nC_m units grafted per HPC chain. On the cellular level, unmodified HPC showed no cytotoxicity, while free POE_nC_m nolecules inhibited cell growth. Most importantly, the study revealed that HPC-*g*-POE_nC_m exhibited no significant cytotoxicity effect[1].

4.2 References

(1) Francis, M. F.; Piredda, M.; Winnik, F. M. *J. Controlled Rel.* **2003**, 93, 59

Acknowledgments

I would like to express my sincere gratitude to Prof. Françoise Winnik for her guidance, suggestions and faith in my potential that made this work realizable.

Thanks are also due to all my colleagues, especially with Mauro, Mariana, Charbel, Julie and Mira. Their friendship makes the year I spent in Montréal very special and unforgettable. I want to thank them for the help and the encouragement ever, but also for the trips, laughs, dinners and activities.

Finally, a heartfelt thanks goes to Marco for his perpetual and unconditional love and support; together we spent a gorgeous and funny time in Montréal: all of this would not have been possible without him.

^{1}H-NMR SPECTRA

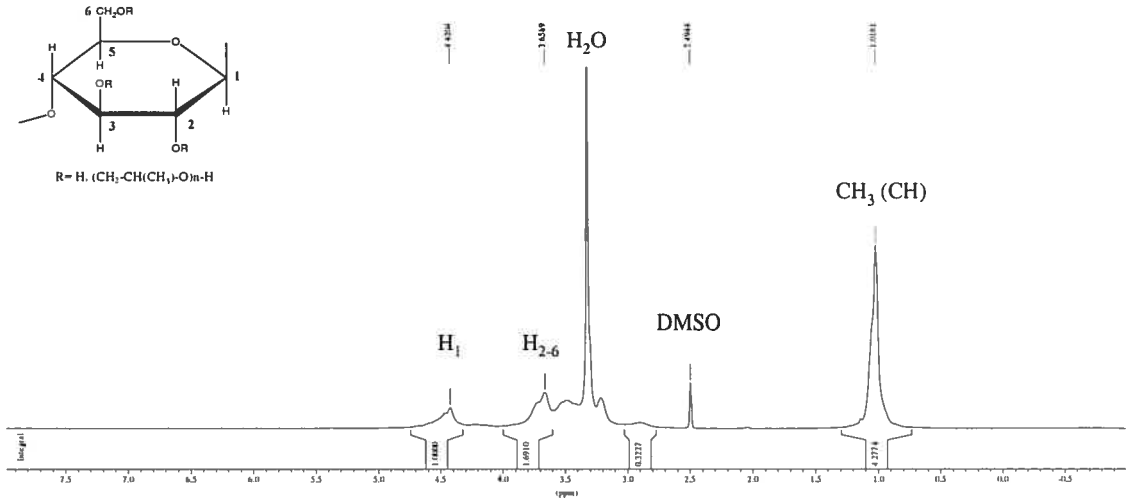

Spectrum 1. HPC in DMSO-d_6

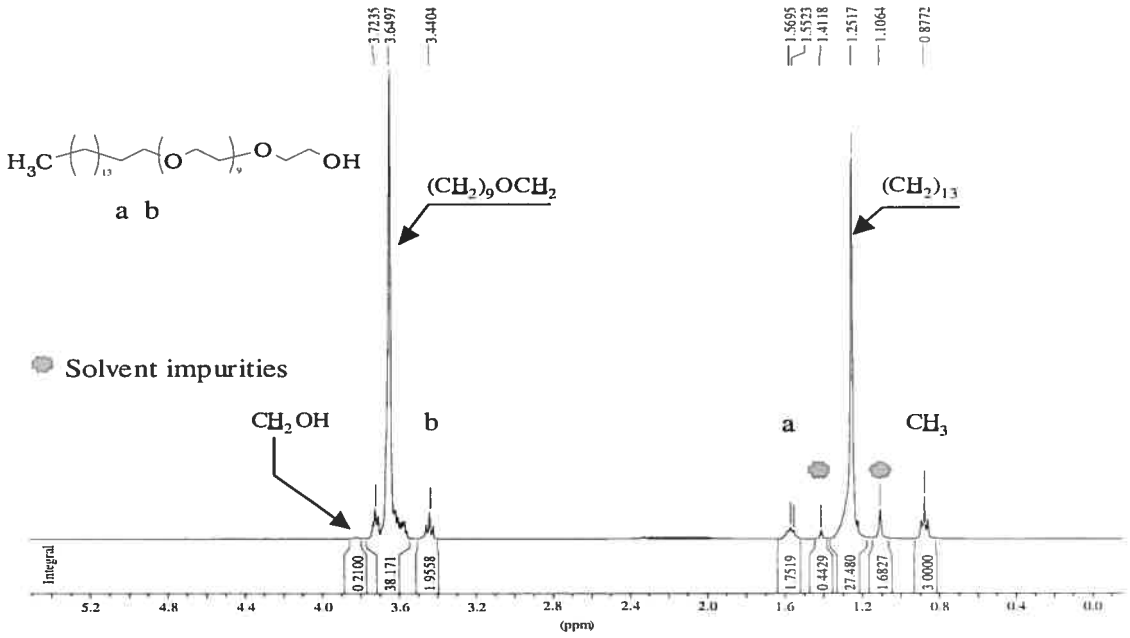

Spectrum 2. $POE_{10}C_{16}$ in $CDCl_3$

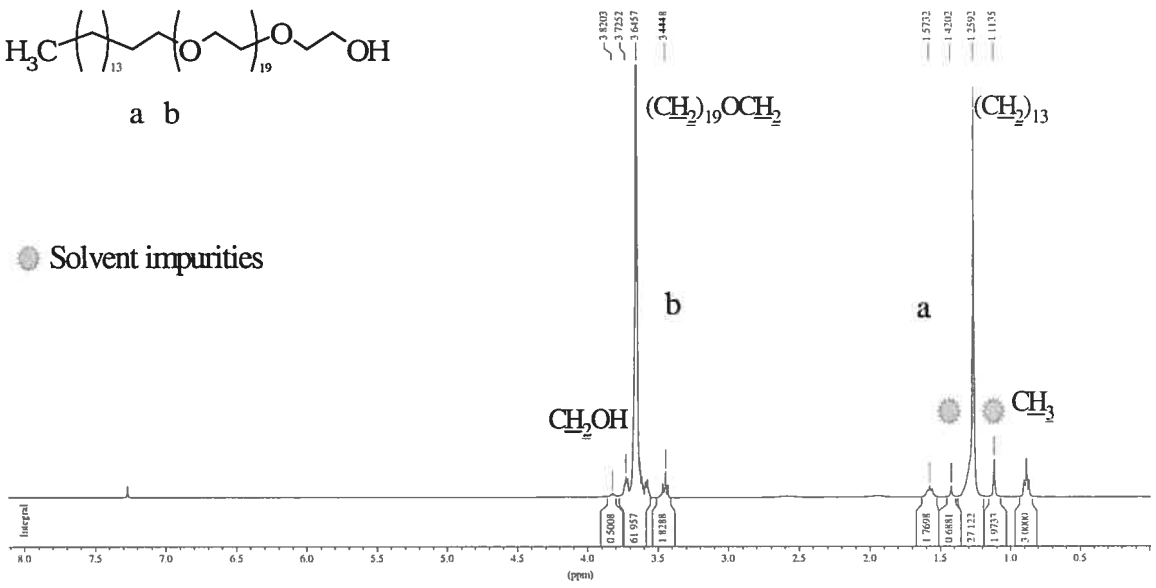

Spectrum 3. $POE_{20}C_{16}$ in $CDCl_3$

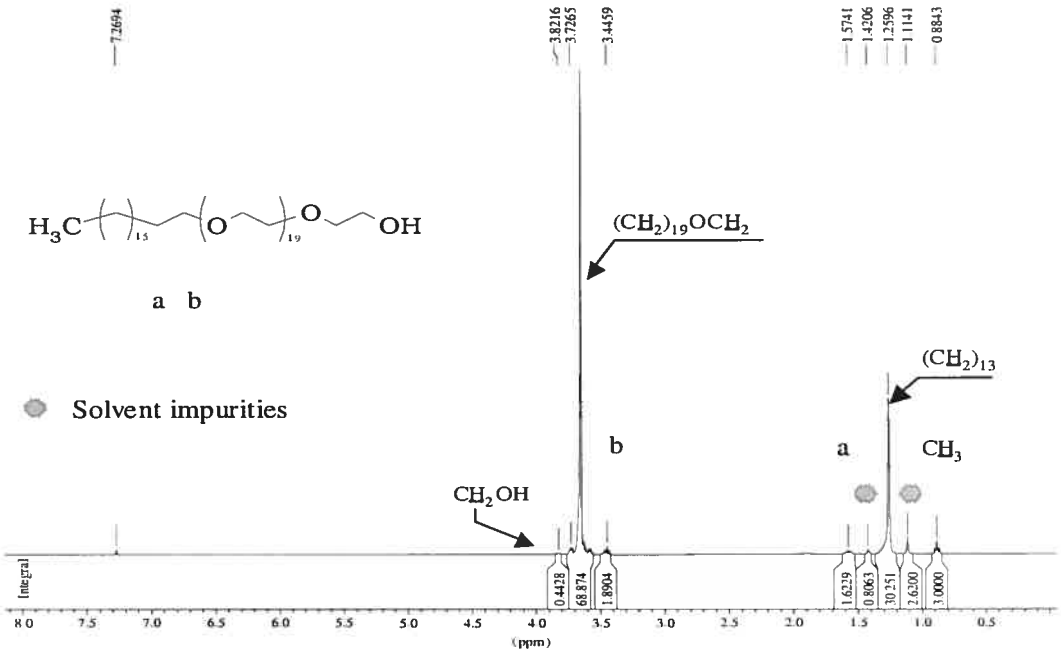

Spectrum 4. $POE_{20}C_{18}$ in $CDCl_3$

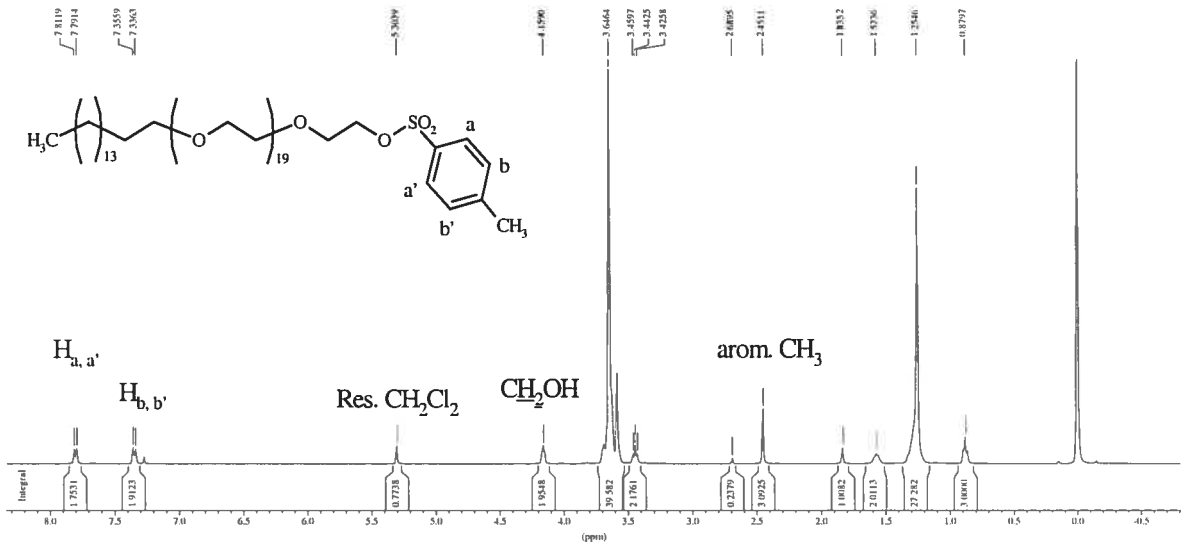

Spectrum 5. $POE_{10}C_{16}$-Tosylate in $CDCl_3$ + TMS as internal standard

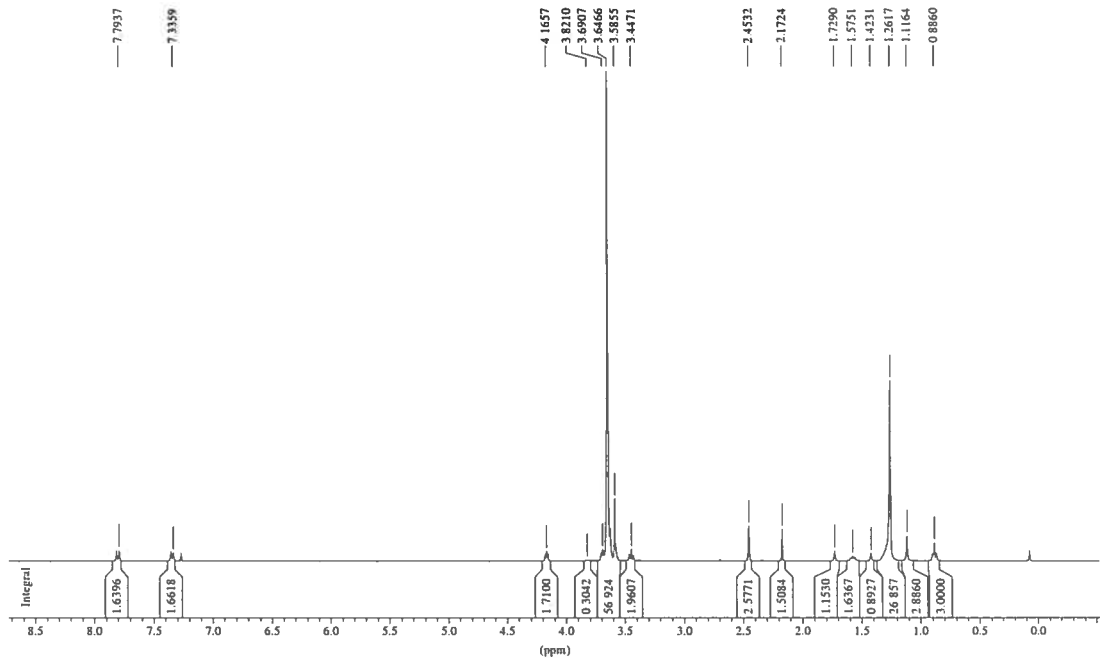

Spectrum 6. $POE_{20}C_{16}$-Tosylate in $CDCl_3$ + TMS as internal standard

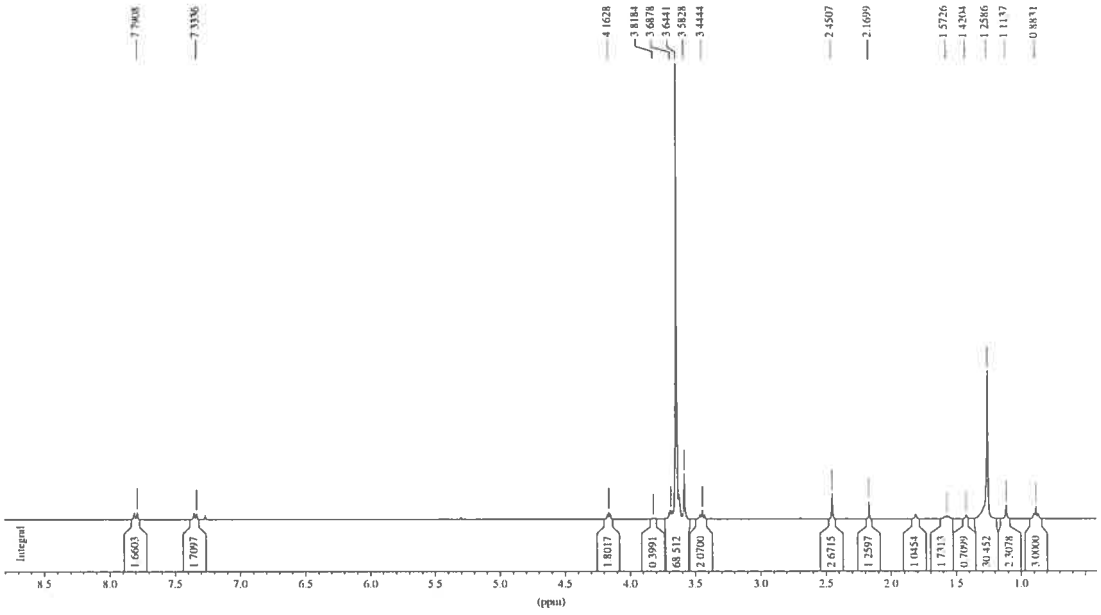

Spectrum 7. $POE_{20}C_{18}$-Tosylate in $CDCl_3$ + TMS as internal standard

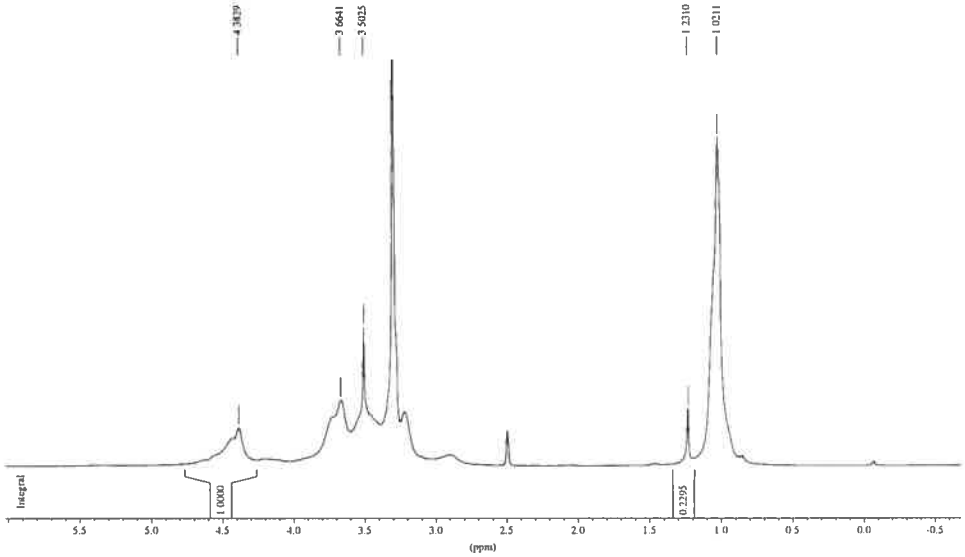

Spectrum 8. HPC-*g*-$POE_{10}C_{16}$ (0.9 % mol) in DMSO-d_6

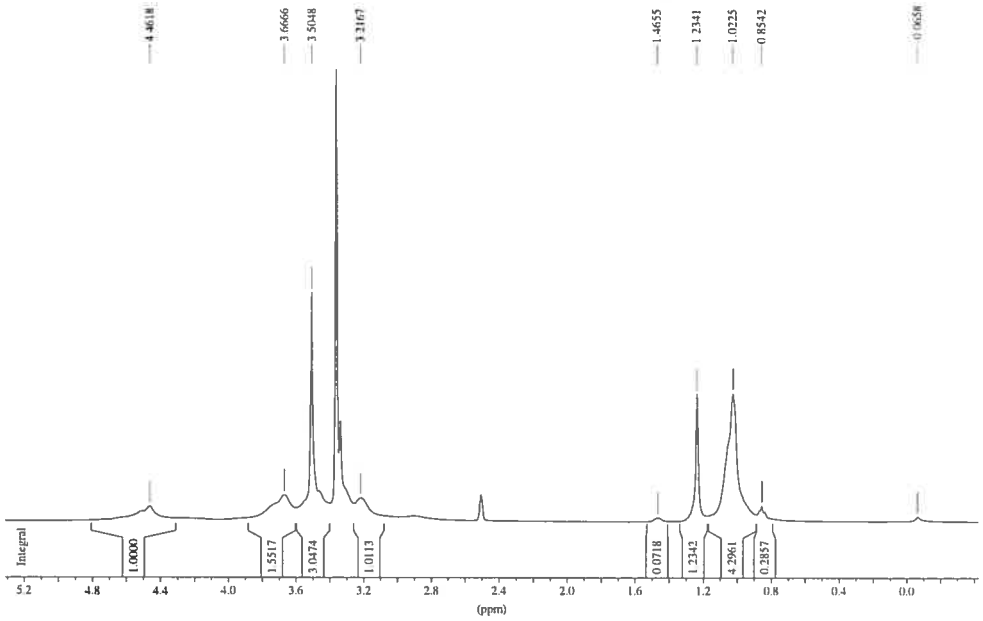

Spectrum 9. HPC-*g*-$POE_{10}C_{16}$ (4.7 % mol) in DMSO-d_6; here POEnCm = $POE_{10}C_{16}$, 2(m-3) = 13, I_a = 1.23, I_a/2(m-3)H x 100 = 4.7%

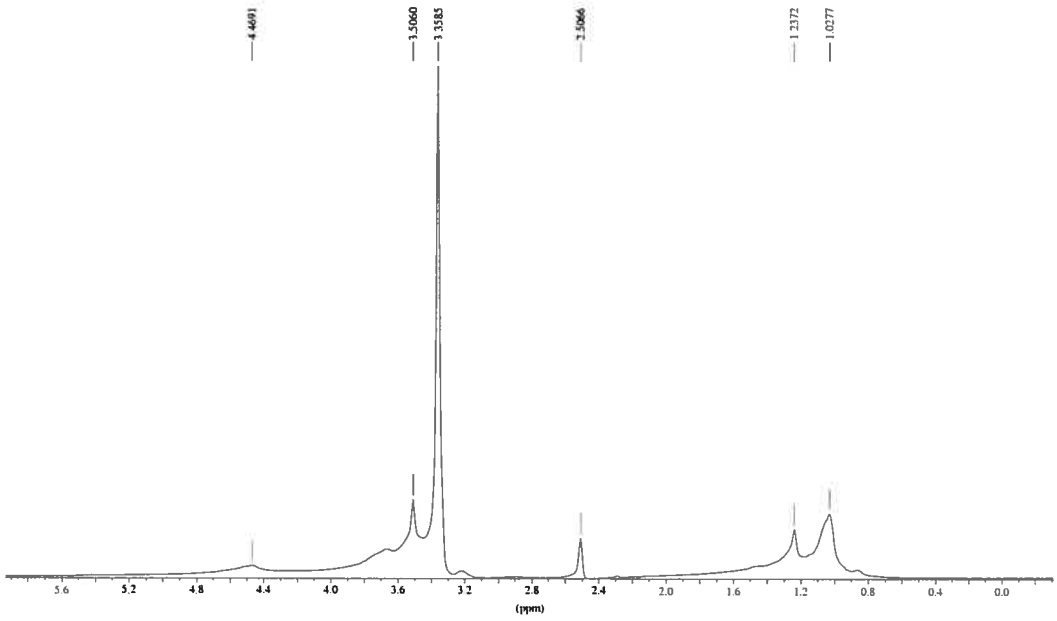

Spectrum 10. HPC-*g*-$POE_{10}C_{16}$ (5.4 % mol) in DMSO-d_6

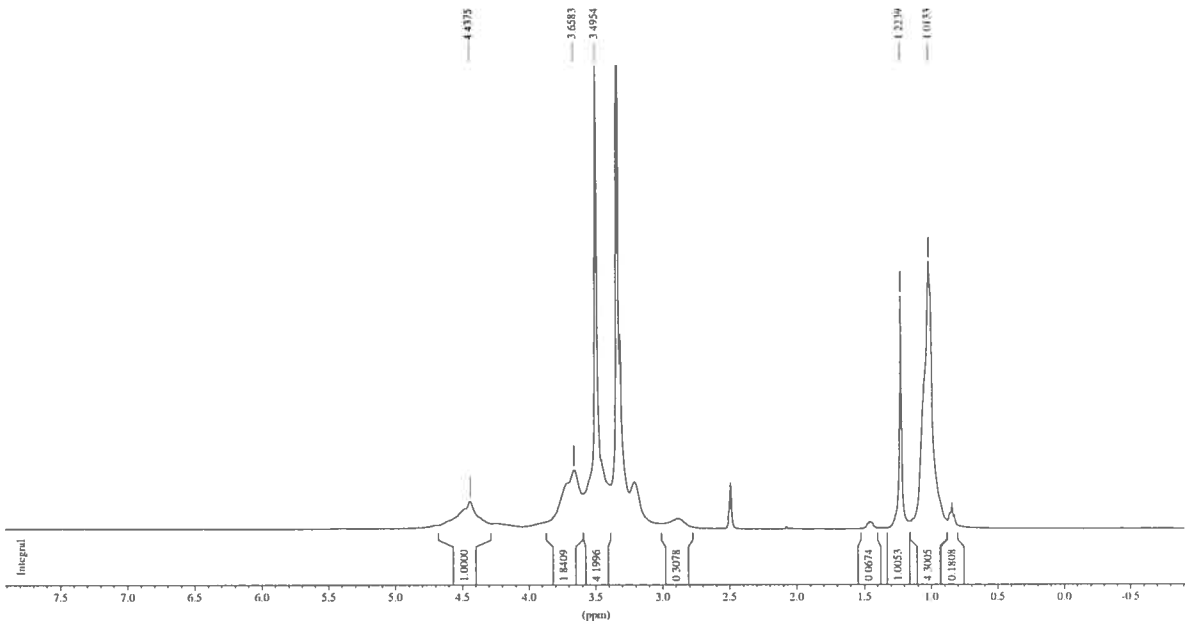

Spectrum 11. HPC-*g*-$POE_{20}C_{16}$ (3.9 % mol) in DMSO-d_6

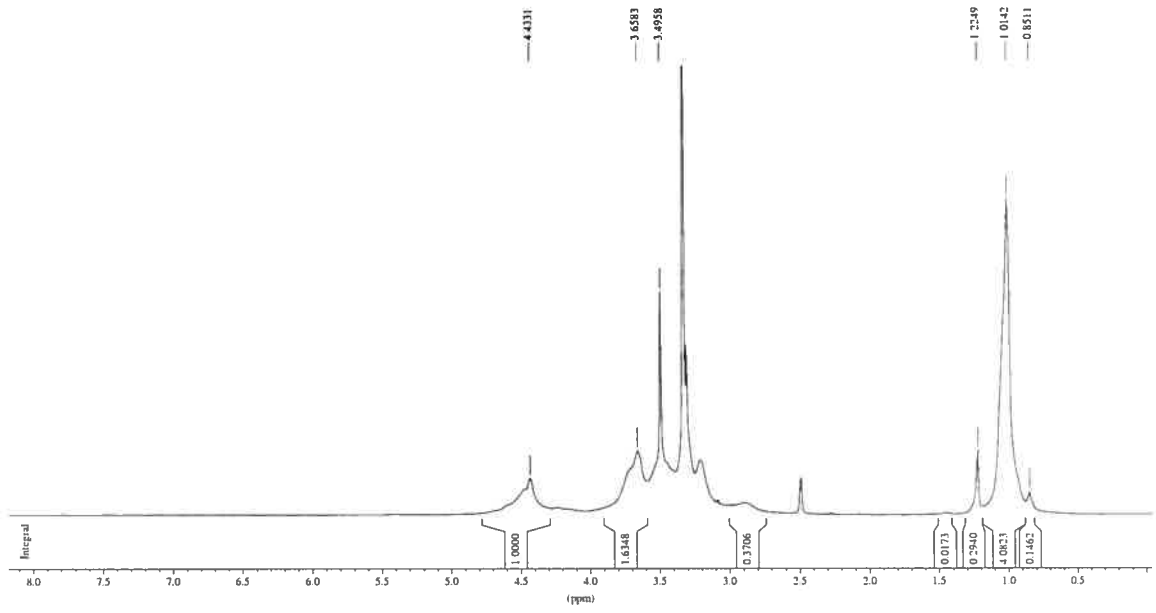

Spectrum 12. HPC-*g*-$POE_{20}C_{16}$ (1.1 % mol) in DMSO-d_6

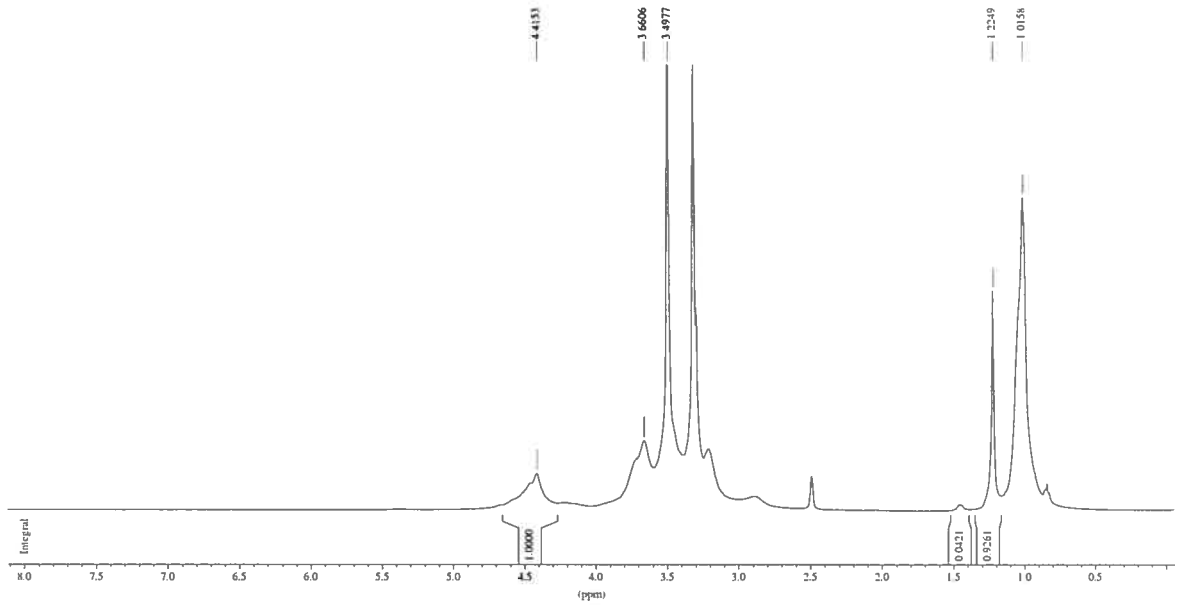

Spectrum 13. HPC-*g*-$POE_{20}C_{18}$ (3.1 % mol) in DMSO-d_6

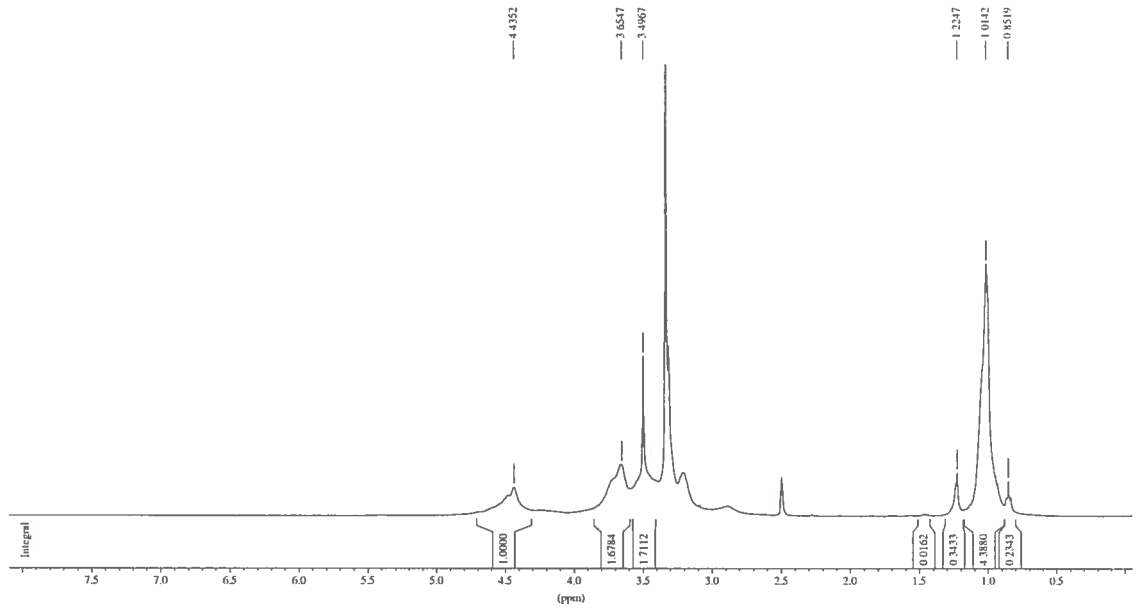

Spectrum 14. HPC-*g*-$POE_{20}C_{18}$ (1.1 % mol) in DMSO-d_6

FLUORESCENCE PLOTS

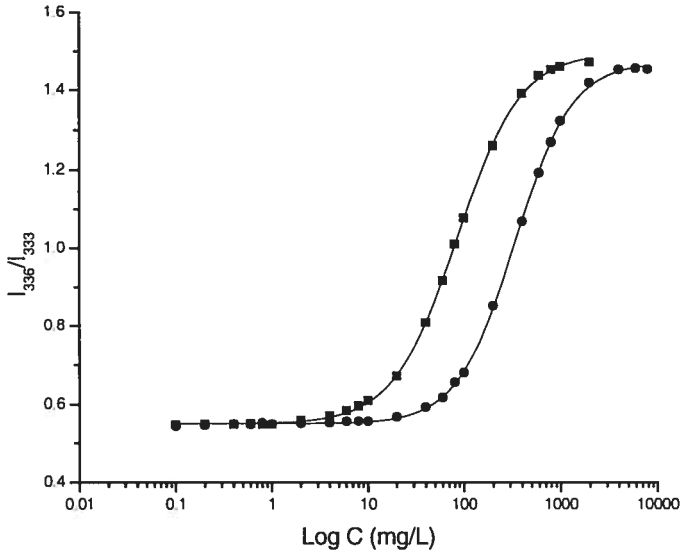

Fluo 1. Plots of pyrene intensity ratio I_{333}/I_{336} as a function of HM-polymer concentration : (■) HPC-$POE_{20}C_{16}$ 3.9%, (●)HPC-$POE_{20}C_{16}$ 1.1%.

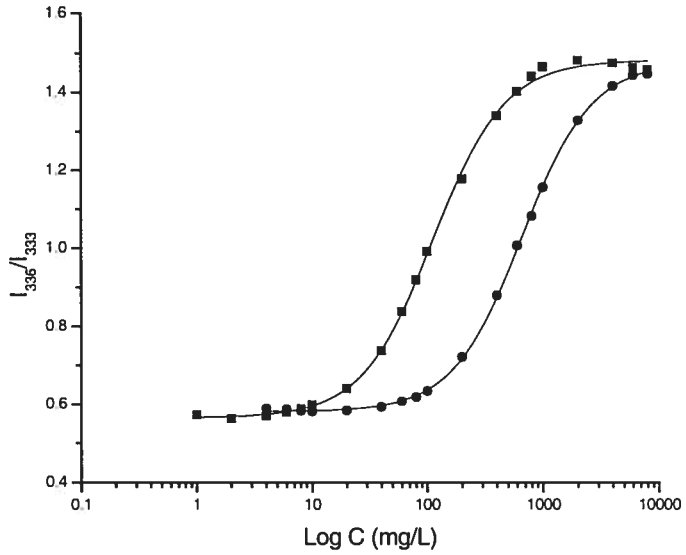

Fluo 2. Plots of pyrene intensity ratio I_{333}/I_{336} as a function of HM-polymer concentration : (■) HPC-$POE_{20}C_{18}$ 3.1%, (●)HPC-$POE_{20}C_{18}$ 1.1%.

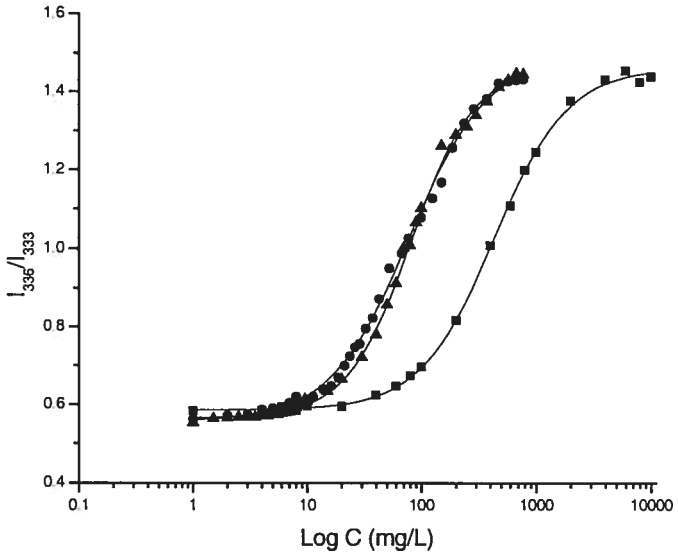

Fluo 3. Plots of pyrene intensity ratio I_{333}/I_{336} as a function of HM-polymer concentration : (■) HPC-$POE_{10}C_{16}$ 0.9%, (▲)HPC-$POE_{10}C_{16}$ 5.4%. (●)HPC-$POE_{10}C_{16}$ 4.7%.

DSC CURVES

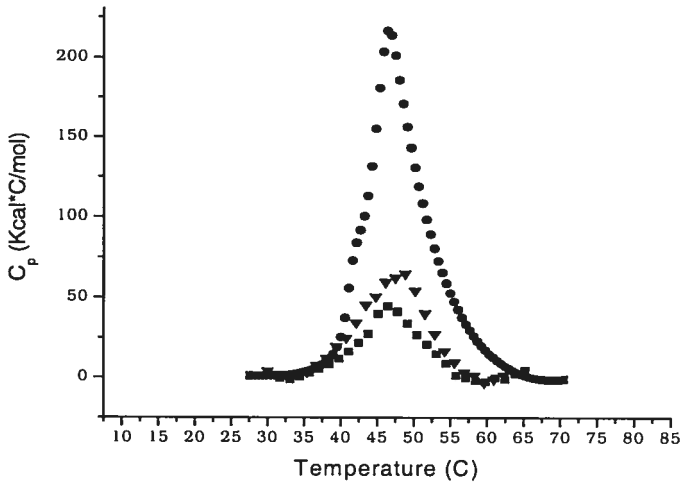

DSC 1. Microcalorimetric endotherms of aqueous solution of HPC-$POE_{10}C_{16}$ with different MS. (●) 0.9 mol%, (▼) 4.7 mol%, (■) 5.4 mol%. 30 °C/hr from 20 °C to 80 °C.

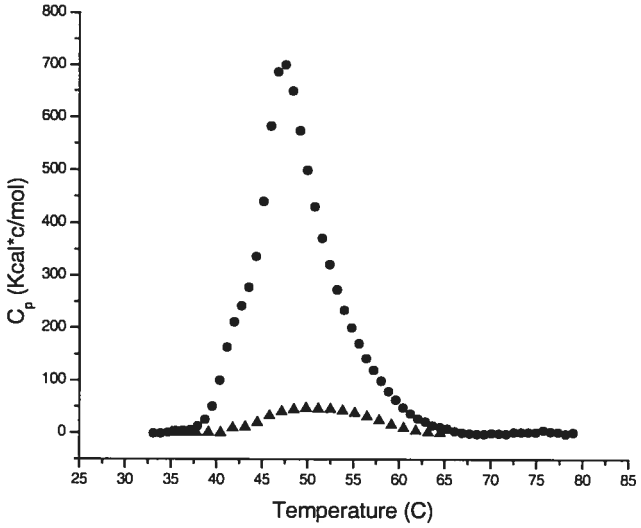

DSC 2. Microcalorimetric endotherms of aqueous solution of HPC-$POE_{20}C_{16}$ with different MS. (●) 1.1 mol%, (▲) 3.9 mol%, 30 °C/hr from 20 °C to 80 °C.

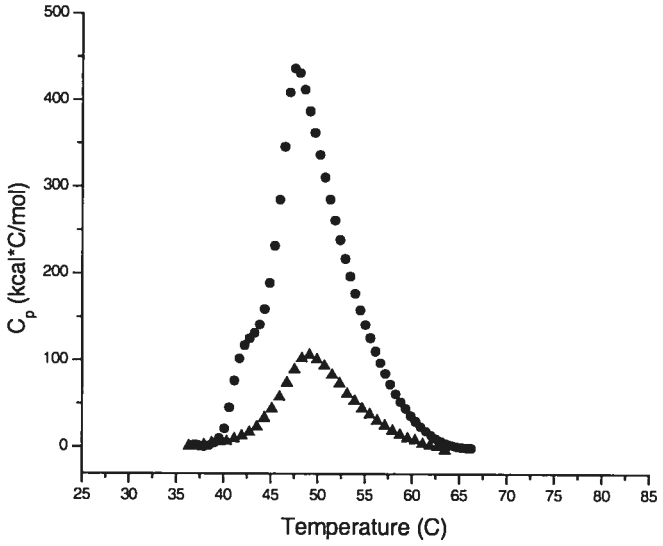

DSC 3. Microcalorimetric endotherms of aqueous solution of HPC-$POE_{20}C_{18}$ with different MS. (●) 1.1 mol%, (▲) 3.1 mol%, 30 °C/hr from 20 °C to 80 °C.